CALIBRATION OF A 200 FT. WAVE TANK AND A STUDY OF THE RESPONSE OF A CIRCULAR CYLINDER TO SINUSOIDAL WAVES

CHUN-MING CHEN

1979

NOTICE

The quality of this microfiche is heavily dependent upon the quality of the original thesis submitted for microfilming. Every effort has been made to ensure the highest quality of reproduction possible.

If pages are missing, contact the university which granted the degree.

Some pages may have indistinct print especially if the original pages were typed with a poor typewriter ribbon or if the university sent us a poor photocopy.

Previously copyrighted materials (journal articles, published tests, etc.) are not filmed.

Reproduction in full or in part of this film is governed by the Canadian Copyright Act, R.S.C. 1970, c. C-30. Please read the authorization forms which accompany this thesis.

THIS DISSERTATION HAS BEEN MICROFILMED EXACTLY AS RECEIVED

AVIS

La qualité de cette microfiche dépend grandement de la qualité de la thèse soumise au microfilmage. Nous avons tout fait pour assurer une qualité supérieure de reproduction.

S'il manque des pages, veuillez communiquer avec l'université qui a conféré le grade.

La qualité d'impression de certaines pages peut laisser à désirer, surtout si les pages originales ont été dactylographiées à l'aide d'un ruban usé ou si l'université nous a fait parvenir une photocopie de mauvaise qualité.

Les documents qui font déjà l'objet d'un droit d'auteur (articles de revue, examens publiés, etc.) ne sont pas microfilmés.

La reproduction, même partielle, de ce microfilm est soumise à la Loi canadienne sur le droit d'auteur, SRC 1970, c. C-30. Veuillez prendre connaissance des formules d'autorisation qui accompagnent cette thèse.

LA THÈSE A ÉTÉ MICROFILMÉE TELLE QUE NOUS L'AVONS REÇUE

CALIBRATION OF A 200 ft WAVE TANK AND A STUDY OF THE RESPONSE OF A CIRCULAR CYLINDER TO SINUSOIDAL WAVES

by

Chun-Ming Chen, B.Sc.

A Thesis submitted in partial fulfillment of the
requirements for the degree of

Master of Engineering

Faculty of Engineering and Applied Science
Memorial University of Newfoundland

December 1978

St. John's Newfoundland

ACKNOWLEDGEMENT

The author wishes to express his gratitude to his supervisor, Dr. D.B. Muggeridge, for his guidance, encouragement, and continuous support throughout the study.

The author wishes to thank Dr. R.T. Dempster, Dean of the Faculty of Engineering and Applied Science for providing the opportunity of carrying out this study. The support and financial assistance of Dr. G. R. Peters, Associate Dean of the Faculty and Ocean Engineering Group Leader is gratefully acknowledged as is the financial support of the National Research Council of Canada(NRC Grant Numbers A8668, A0820). The generous financial support offered by Memorial University of Newfoundland is gratefully acknowledged. Thanks are due to Dr. F.A. Aldrich, Dean of the School of Graduate Studies, and Professor N.W. Wilson, Chairman, Graduate Studies Committee, Faculty of Engineering and Applied Science, for their support. The kind assistance of Mr. G. Langlois, Mr. J. Dutton, and Mr. J. Murray is also appreciated.

ABSTRACT

A series of experiments have been carried out to verify linear wave generator theory as well as to study wave forces on a vertical circular cylinder. The experimental data shows that linear wave generator theory can accurately predict the relationship between water depth, stroke of the wave generator, wave height, and wave period. Experimental forces and overturning moments on the cylinder show reasonably good agreement with linear wave theory and Morison's equation.

TABLE OF CONTENTS

NOMENCLATURE

a	amplitude of the incident wave
a_i	modal coefficient
A	projected area perpendicular to the stream velocity
b	width of the wave tank
C_D	drag coefficient
C_L	lift coefficient
C_M	mass coefficient
d	still water depth
d/L	relative depth
D	cylinder diameter
D/L	relative diameter
e	stroke of the wave generator (one-half its total motion)
E	Elastic modulus
f	wave frequency, $1/T$
f_1	fundamental frequency of the cylinder
f_i	natural frequencies of the cylinder
f_v	vortex shedding frequency
F_D	drag force
F_I	inertia force
F_L	lift force
$F_h(s)$	horizontal longitudinal force on a differential length ds of the cylinder
F_h	total horizontal longitudinal force

$F_T(s)$	horizontal transverse force on a differential length ds of the cylinder
F_T	total horizontal transverse force
g	acceleration due to gravity
H	wave height
H/L	wave steepness
I	moment of inertia
k	wave number, $2\pi/L$
K	attenuation coefficient
ℓ	cylinder length
L	wavelength
m	cylinder mass
m_w	added-mass of the water
MF_h	total horizontal longitudinal force(experimental)
MF_T	total horizontal transverse force(experimental)
M_{S_1}	total longitudinal moment about any point S_1 on the cylinder
MM_{S_1}	M_{S_1} (experimental)
M_{ST}	total transverse moment about any point S_1 on the cylinder
MM_{ST}	M_{ST} (experimental)
Re	Reynolds number, $u_{max}\ D/\nu$
S	Strouhal number, $f_v\ D/u_{max}$
t	time
T	wave period
u	horizontal component of the water particle velocity

u_{max}	maximum horizontal water particle velocity
$u_{max}\,T/D$	Keulegan-Carpenter number
v	vertical component of the water particle velocity
x	horizontal distance from the wave crest
X	horizontal distance from mean position of the wave generator
y	vertical distance from the still water level to the water particle
β_{hf}	phase angle of the maximum total horizontal longitudinal force
β_{hm}	phase angle of the maximum total longitudinal moment
β_{hT}	phase angle of the maximum total horizontal transverse force
δ	unknown phase angle
ε_r	reflection coefficient
μ	Poisson's ratio
ν	kinematic viscosity of fluid
ρ	mass density of water
σ	circular wave frequency, $2\pi/T$
$\partial u/\partial t$	horizontal component of the water particle local acceleration

LIST OF TABLES

LIST OF FIGURES

LIST OF FIGURES-Continued

1. INTRODUCTION

This thesis consists of two parts; one deals with the calibration of a 200 ft x 15 ft x 10 ft (61 m x 4.57m x 3 m) wave tank, the other deals with wave forces on a vertical circular cylinder due to sinusoidal waves.

Experiments designed to verify the theoretical prediction of wave heights in terms of the stroke of the wave generator, water depth, and wave period were performed at Laboratoire Neyrpic (1952). Waves were generated by a paddle-type wave generator and the measured wave height at some distance from the wave generator was consistently about 30% below theoretical predictions. Ursell et al.[27] verified the linear wave generator theory by using a piston-type wave generator for a series of tests. When the wave steepness was within the range of $0.002 \leq H/L \leq 0.03$, the measured wave heights were 3.4% below the theoretical predictions. The measured wave heights were 10% below the theoretical prediction when the range of wave steepness was $0.045 \leq H/L \leq 0.048$. Therefore, the experiments verified the validity of the small-amplitude wave theory.

Madsen, Tenney, Keating and Webber[13] also studied waves using a piston-type wave generator. Madsen's results gave measured wave heights that were 15% below the theory. Tenney's experiments, in which two holes were drilled through the waveboard, indicated a difference of 3% between the two cases (holes open and closed). Keating and Webber measured wave heights in the range of $0.005 \leq H/L \leq 0.08$ which were 6% below theoretical predictions if leakage around the wave generator could be eliminated. They concluded that linear wave generator theory was more applicable to shallow water waves than deep water waves.

The present experiments show good agreement, in the range of $0.0012 \leq H/L \leq 0.0876$, with linear wave generator theory for a piston-type wave generator.

Horizontal wave forces on a vertical circular cylinder which extends from the ocean bottom and pierces through the water surface are made up of two components. One is the longitudinal force in the direction of wave propagation, the other is the transverse force normal to the direction of wave propagation.

If the diameter of the cylinder is small compared with the wavelength ($D/L < 0.1$), the longitudinal force is normally calculated by using Morison's equation which consists of a drag force and an inertia force. The transverse force due to vortex shedding from the cylinder, under certain circumstances, is not negligible. Wiegel, et al.[29] studied wave forces on piles and showed that large lateral oscillations could occur.

Jen[12] studied wave forces due to uniform periodic waves on the basis of linear wave theory in the ranges of $d/L > 0.175$, $H/L < 0.02$, and $D/L \leq 0.12$. He found out that inertia forces were predominant and that the coefficient C_M had an overall average of 2.04. Morison et al.[21] presented data using small amplitude wave theory for $0.102 < d/L < 0.529$, $0.009 < H/L < 0.1135$, and $0.009 < D/L < 0.0419$. He found out that $C_M = 1.508 \pm 0.197$ and that $C_D = 1.626 \pm 0.414$ (for $2.2 \times 10^3 \leq Re \leq 1.11 \times 10^4$).

The experimental values of C_D and C_M were computed from the measured total moment in order to calculate the measured force; theoretical moment and force. In Jen's experiment, the drag forces on the circular pile were

so small that he assumed C_D to be zero and measured C_M. Wiegel et al.[29] calculated C_D when the acceleration was zero and C_M when the velocity was zero.

Wiegel et al.[29] showed that there was no relationship between C_M and Re. Morison et al.[21] presented results showing that C_M and C_D were not dependent upon Re (for $2.2 \times 10^3 \leq Re \leq 1.11 \times 10^4$). Wiegel[28] thought that the Keulegan-Carpenter number in terms of C_D and C_M was more significant than Re. Keulegan and Carpenter[7] stated that C_D and C_M were functions not of Re but of the Keulegan-Carpenter number. More recently it has been reported that both C_D and C_M are dependent on Re and Keulegan-Carpenter number[2,7].

Bidde[1] showed that the transverse force was not dependent on Re but rather was a function of the Keulegan-Carpenter number. However, Isaacson and Maull[10] stated that the transverse forces were functions of Re and Keulegan-Carpenter number, and transverse forces occur when the Keulegan-Carpenter number had a value of 5 on the surface of the flow.

Jen[12], Mogridge and Jamieson[20], and Bidde[1] all report results of experimental investigations into wave forces on cylinders. They used a vertical circular cylinder in which the lower end of the cylinder was not in contact with the bottom of the tank. The present experiment, in which the cylinder is fixed on the bottom of the tank and wave forces and moments are measured over several ranges of wave parameters, yields reasonably good agreement with linear wave theory.

2. WAVE TANK CALIBRATION

2.1 Wave Generating System

The wave tank is a reinforced concrete structure which is 200 ft long, 15 ft wide and 10 ft deep, and has glass panels on one side near the test section, as shown in Figure 1. It is provided with a MTS closed-loop, servo-hydraulic wave generator (see Figure 2) which is capable of generating sinusoidal or programmed waves. Waves are produced by the translatory motion of a waveboard which is driven by the hydraulic actuator, as shown in Figure 3. The servo-valve regulates actuator stroke in response to the control signal developed in the servo controller. The servo controller develops the error signal by comparing its command and feedback. The waveboard position is automatically maintained at the command level. A block diagram of a position control servo loop is shown in Figure 4.

A beach of slope 1:6.2 (around 9°), as shown in Figure 5, is constructed of 5 modules each consisting of orthogonal wooden grids mounted on top of plywood. Each module may be varied in elevation and slope. Figure 6 shows the layout of the wave tank.

Each wave probe is of the resistance type consisting of a pair of parallel stainless steel wires, 0.059 in. in diameter, 19.69 in. in length and spaced 0.49 in. apart. The wave probes are calibrated in still water by raising and lowering them by known increments. The output of each probe was recorded on magnetic tape and on a strip chart recorder.

2.2 Wave Generator Performance

The closed loop servo-hydraulic wave generator is designed to generate wave forms within the wave height to wavelength performance envelope, at different water depth, on the basis of Biesel's equation

for a piston-type wave generator. Biesel's equation (linear wave generator theory) is defined as:

$$\frac{H}{e} = \frac{4 \sinh^2 (\frac{2\pi d}{L})}{\sinh (\frac{2\pi d}{L}) \cosh(\frac{2\pi d}{L}) + \frac{2\pi d}{L}} \qquad (1)$$

where e is the stroke of the wave generator.

Two wave probes were installed about 35 ft. apart near the middle of the wave tank to measure the wave height and wave length. The wave height to wave length performance envelope was then established by varying the stroke of the wave generator from 0.5 in to 10 in, at frequencies of 0.2 Hz to 1 Hz with 4.5 ft and 3 ft water depths as shown in Figures 7 and 9. The computer program based on the Biesel's equation for the analysis of the piston-type wave generator is listed in Appendix A.

2.3 Reflection Coefficient of the Beach

When a primary incident wave travels toward the beach, it will be partially reflected and partially absorbed by the beach. Successive reflections occur until steady state is established. A partial standing wave system is thus established along the length of the wave tank. Therefore, the wave heights are not the same at all points but vary as a function of the distance from the wave generator[27].

$$H = 2a[1 + \varepsilon_r \cos(2kx_1 + \delta) + \varepsilon_r \cos \delta] \qquad (2)$$

That is, the wave height variation is a sinusoidal oscillation with a wavelength which is approximately equal to one-half the wavelength of the incident wave.

The definition of the reflection coefficient ε_r of the beach is the ratio of the reflected wave height (H_r) to the incident wave height (H_i).

If the maximum and minimum values of the sinusoidal variation in wave height are denoted by H_{max} and H_{min}, respectively, then the reflection coefficient may be expressed as:

$$\epsilon_r = \frac{H_r}{H_i} = \frac{H_{max} - H_{min}}{H_{max} + H_{min}} \tag{3}$$

Seven wave probes spaced 2 ft. apart, the first being located 48 ft from the mean position of the wave generator in the wave tank were used to measure reflection coefficients.(see Fig. 13).

2.4 Wave Attenuation Coefficient

When wave heights are measured in a finite width wave tank, the viscosity of the boundary layer on the side walls and bottom of the tank causes a slight attenuation of the wave height due to energy dissipation in the wave propagation. A theoretical estimation of the attenuation coefficient K is defined as[27]

$$K = \frac{2k}{b}\left(\frac{\nu}{2\sigma}\right)^{1/2}\left(\frac{kb + \sinh 2kd}{2kd + \sinh 2kd}\right) \tag{4}$$

where b is the width of the wave tank, ν is the kinematic viscosity, k is the wave number and σ is $\frac{2\pi}{T}$.

Suppose that two wave probes are located 61.8 ft apart near the middle of the wave tank to avoid the wave generator and beach effects and the individual wave heights H_1 and H_2 are measured. Then the attenuation coefficient can be determined by:

$$H_2 = H_1 e^{-K(X_2 - X_1)} \tag{5}$$

where $X_2 - X_1 = 61.8$ ft.

Obviously, the decrease in the wave height is so small that it can be neglected from a practical point of view. The theoretical and measured wave attenuation coefficient are shown in Table 3.

2.5 Discussion of Results

A series of tests were performed in order to verify linear wave generator theory. This theory predicts the relationship between the wave height, wave period, water depth and the stroke of the wave generator for a piston-type wave generator.

Measured values of H and L, H/e and $2\pi d/L$, for 4.5 ft and 3 ft water depths oven the range of $0.074 < d/L < 0.6977$, $0.0012 < H/L < 0.0876$ and $0.058 < d/L < 0.548$, $0.0012 < H/L < 0.1$ respectively are compared with those obtained from equation (1) in Figures 7-12 and Tables 1 and 2. The wavelength might be considered as a constant throughout the entire range of strokes of the wave generator at the same wave period as it has a maximum standard deviation of 1.38 and 0.58 for 4.5 ft and 3 ft water depths respectively. The wave generator can generate a maximum wave height of 1.343 ft having a corresponding wavelength of 13.35 ft. The maximum wave steepness is 1/10. The wave height to wavelength performance envelopes for the 3 ft water depth, as shown in Figures 9 and 10, have a better agreement with linear wave generator theory than the wave height to wavelength performance envelopes for the 4.5 ft water depth, as shown in Figures 7-8.

The experimental results in the range of the small amplitude waves $0.0012 < H/L < 0.03$ (Figures 11 and 12) show better agreement with theory than in the range of the finite amplitude waves $0.03 < H/L < 0.0876$ and $0.03 < H/L < 0.1$ for both 4.5 ft and 3 ft water depths respectively.

However, all the experimental results for a 3 ft water depth are closer to the theory than those results obtained for the 4.5 ft water depth. A variety of factors could account for the difference. Errors in measurement of wave height, wavelength, water depth, and wave generator stroke; some effects such as interference due to transverse reflection from the side walls of the wave tank; leakage around the waveboard; motion of the waveboard which is not quite simple harmonic; and lack of a perfect wave energy absorber.

The wave height variation with distance along the wave tank is a sinusoidal oscillation which has a wavelength approximately equal to one-half the wavelength of the incident wave. The reflection coefficient is less than 10%. The attenuation coefficient of the wave height due to viscous boundary layers is so small that it can be neglected from a practical standpoint, as shown in Table 3.

3. RESPONSE OF A VERTICAL CIRCULAR CYLINDER TO SINUSOIDAL WAVES

3.1 Wave Induced Forces and Overturning Moments

Morison's equation for the wave forces due to potential flow on a submerged vertical cylinder for which the ratio of cylinder diameter to wavelength is very small consists of two components. One is a drag force due to the water particle velocity, the other is an inertia force due to the water particle acceleration. These coefficients may be determined experimentally. It is assumed that the flow is inviscid, incompressible, and irrotational. Furthermore, the ratio of wave height to wave length is so small that linear wave theory can be applied. The inertia force on the submerged vertical circular cylinder may be expressed as

$$F_I = C_M \rho \left(\frac{\pi D^2}{4}\right) \frac{\partial u}{\partial t} \qquad (6)$$

The drag force which consists of both frictional drag and form drag on the submerged vertical circular cylinder may be expressed as

$$F_D = \frac{1}{2} C_D \rho A u^2 \qquad (7)$$

Morison, O'Brien and Johnson (1950)[21] combined the inertia force and drag force to obtain the total force expressed as

$$F = F_I + F_D = C_M \rho \left(\frac{\pi D^2}{4}\right) \frac{\partial u}{\partial t} + \frac{1}{2} C_D \rho A |u| u \qquad (8)$$

where the horizontal components of velocity and local acceleration are given by:

$$u = \frac{\pi H}{T} \frac{\cosh[2\pi(y+d)/L]}{\sinh 2\pi d/L} \cos 2\pi\left(\frac{x}{L} - \frac{t}{T}\right) \qquad (9)$$

$$\frac{\partial u}{\partial t} = \frac{2\pi^2 H}{T^2} \frac{\cosh[2\pi(y+d)/L]}{\sinh 2\pi d/L} \sin 2\pi\left(\frac{x}{L} - \frac{t}{T}\right) \tag{10}$$

where $x,t = 0$ defines the wave crest to be at the centre of the cylinder.

The horizontal force $F_h(s)$ on a differential length of a vertical circular cylinder ds, as shown in Figure 13, is given by [28]

$$F_h(s) = \left[C_M \rho \left(\frac{\pi D^2}{4}\right) \frac{\partial u}{\partial t} + \frac{1}{2} C_D \rho D |u| u\right] ds \tag{11}$$

It is assumed that C_D and C_M are constant for the entire length of the cylinder. The total horizontal force on the cylinder between two points S_1 and S_2 where $S_2 < S_s$ (the surface) is given by:

$$F_h = \int_{S_1}^{S_2} F_h(s) = \int_{S_1}^{S_2} \left[C_M \rho \left(\frac{\pi D^2}{4}\right) \frac{\partial u}{\partial t} + \frac{1}{2} C_D \rho D |u| u\right] ds$$

$$= \pi \rho D \frac{H^2 L}{T^2} \left[\frac{\pi D}{4H} C_M K_2 \sin 2\pi\left(\frac{x}{L} - \frac{t}{T}\right) + C_D K_1 \left|\cos 2\pi\left(\frac{x}{L} - \frac{t}{T}\right)\right| \cos 2\pi\left(\frac{x}{L} - \frac{t}{T}\right)\right], \tag{12}$$

where $$K_1 = \frac{\frac{4\pi S_2}{L} - \frac{4\pi S_1}{L} + \sinh \frac{4\pi S_2}{L} - \sinh \frac{4\pi S_1}{L}}{16\left(\sinh \frac{2\pi d}{L}\right)^2} \tag{13}$$

$$K_2 = \frac{\sinh \frac{2\pi S_2}{L} - \sinh \frac{2\pi S_1}{L}}{\sinh \frac{2\pi d}{L}} \tag{14}$$

By differentiating equation (12) with respect to $2\pi\left(\frac{x}{L} - \frac{t}{T}\right)$ and

setting the derivative $dF_h/d[2\pi(x/L-t/T)]$ equal to zero, the phase angle β_{hf} of the maximum total horizontal force can be obtained,

$$\sin \beta_{hf} = \pm \frac{\pi D C_M K_2}{8HC_D K_1} \tag{15}$$

If $\sin\beta_{hf} > 1$, then $\cos\beta_{hf} = 0$; that is, the wave crest (or trough) lags behind the force by $\pi/2$. (see Ref. 28)

The total longitudinal moment about any point S_1 on the vertical circular cylinder is given:

$$M_{S_1} = \int_{S_1}^{S_2} (S - S_1)\, dF_h$$

$$= \rho D \left(\frac{HL}{T}\right)^2 \left\{\frac{\pi D}{4H} C_M K_4 \sin 2\pi\left(\frac{x}{L} - \frac{t}{T}\right) + C_D K_3 \left|\cos 2\pi\left(\frac{x}{L} - \frac{t}{T}\right)\right| \cos 2\pi\left(\frac{x}{L} - \frac{t}{T}\right)\right.$$

$$\left. - \frac{2\pi S_1}{L}\left[\frac{\pi D}{8H} C_M K_2 \sin 2\pi\left(\frac{x}{L} - \frac{t}{T}\right) + \frac{1}{2} C_D K_1 \left|\cos 2\pi\left(\frac{x}{L} - \frac{t}{T}\right)\right| \cos 2\pi\left(\frac{x}{L} - \frac{t}{T}\right)\right]\right\} \tag{16}$$

where K_1 and K_2 are same as equations (13) and (14).

$$K_3 = \frac{\frac{1}{2}\left(\frac{4\pi S_2}{L}\right)^2 - \frac{1}{2}\left(\frac{4\pi S_1}{L}\right)^2 + \frac{4\pi S_2}{L}\sinh\frac{4\pi S_2}{L} - \frac{4\pi S_1}{L}\sinh\frac{4\pi S_1}{L} - \cosh\frac{4\pi S_2}{L} + \cosh\frac{4\pi S_1}{L}}{64\left(\sinh\frac{2\pi d}{L}\right)^2} \tag{17}$$

$$K_4 = \frac{\frac{2\pi S_2}{L}\sinh\left(\frac{2\pi S_2}{L}\right) - \frac{2\pi S_1}{L}\sinh\frac{2\pi S_1}{L} - \cosh\frac{2\pi S_2}{L} + \cosh\frac{2\pi S_1}{L}}{2\sinh\left(\frac{2\pi d}{L}\right)} \tag{18}$$

By differentiating equation(16)with respect to $2\pi(\frac{x}{L} - \frac{t}{T})$ and setting the derivative $dM_{S_1}/d\{2\pi(x/L-t/T)\}$ equal to zero, the phase angle β_{hm} of the maximum total longitudinal moment at S_1 can be obtained.

$$\sin\beta_{hm} = \pm \frac{\pi D C_M\left[K_4 - \left(\frac{2\pi S_1}{L}\right)\left(\frac{K_2}{2}\right)\right]}{8HC_D\left[K_3 - \left(\frac{2\pi S_1}{L}\right)\left(\frac{K_1}{2}\right)\right]} \tag{19}$$

If $\sin\beta_{hm} > 1$, then $\cos\beta_{hm} = 0$; that is, the wave crest (or trough) lags behind the moment by $\pi/2$. (see Ref. 28)

The transverse force, due to vortex shedding as the waves pass the vertical circular cylinder, may be expressed as

$$F_L = \frac{1}{2} C_L \rho u^2 A \tag{20}$$

and the transverse force $F_T(s)$ on a differential length of a vertical circular cylinder ds is given

$$F_T(s) = \left[\frac{1}{2} C_L \rho u^2 D\right] ds \tag{21}$$

Assuming that C_L is a constant for the entire length of the cylinder, the total transverse force on the cylinder between S_1 and S_2 is given

$$F_T = \int_{S_1}^{S_2} F_T(s) = \int_{S_1}^{S_2} \frac{1}{2} C_L \rho u^2 D \, ds = \frac{C_L \rho D \pi H^2 L K_1}{T^2} \{\cos 2\pi(\frac{x}{L} - \frac{t}{T})\}^2 \qquad (22)$$

where K_1 is same as equation (13).

By differentiating equation (22) with respect to $2\pi(x/L - t/T)$ and setting the derivative $dF_T/d\{2\pi(x/L - t/T)\}$ equal to zero, the phase angle β_{hT} of the maximum total horizontal transverse force can be obtained.

$$\sin 2\beta_{hT} = 0 \qquad (23)$$

therefore $\beta_{hT} = 0^o$ or $\pi/2$.

$$\text{Therefore, } F_{Tmax} = \frac{C_L \rho D \pi H^2 L K_1}{T^2} \qquad (24)$$

$$\text{or } F_{Tmin} = 0$$

The total transverse moment about any point S_1 on the vertical circular cylinder is given

$$M_{ST} = \int_{S_1}^{S_2} (S - S_1) \, dF_T$$

$$= C_L \rho D (\frac{HL}{T})^2 (K_3 - \frac{\pi S_1}{L} K_1) \{\cos 2\pi(\frac{x}{L} - \frac{t}{T})\}^2 \qquad (25)$$

where K_1 and K_3 are same as equations (13) and (17).

By differentiating equation (25) with respect to $2\pi(x/L - t/T)$ and setting the derivative $dM_{ST}/d\{2\pi(x/L - t/T)\}$ equal to zero, the phase angle β_{MST} of the maximum total transverse moment at S_1 can be obtained.

$$\sin 2\beta_{MST} = 0 \qquad (26)$$

therefore $\beta_{MST} = 0^o$ or $\pi/2$.

Therefore, when $\beta_{MST} = \pi/2$, $M_{ST} = 0$ is the minimum value; when $\beta_{MST} = 0^{\circ}$,

$$M_{ST} = C_L \rho D \left(\frac{HL}{T}\right)^2 \left(K_3 - \frac{2\pi S_1}{L} \frac{K_1}{2}\right) \tag{27}$$

3.2 Keulegan-Carpenter Number and Reynolds Number

There are two nondimensional numbers, Reynolds number and Keulegan-Carpenter number, which are related to wave forces and drag, inertia, and lift coefficients. C_D is a function of Re in steady flow. Hogben et al.[7] have shown that C_D decreased with increasing Re in steady flow (for $5\times10^4 \leq Re \leq 5\times10^5$). For a small diameter cylinder C_D, C_M, and C_L depend on $u_{max}T/D$. Keulegan and Carpenter have shown that C_D and C_M of the circular cylinder were functions of $u_{max}T/D$. When $u_{max}T/D$ is small, separation of flow from the cylinder doesn't occur; when $u_{max}T/D$ is relatively high, a Karman vortex street is formed.

The definitions of Keulegan-Carpenter number and Reynolds number may be expressed as

$$\text{Keulegan-Carpenter number} = \frac{u_{max}T}{D} = \frac{\pi H \cosh\{2\pi(y+d)/L\}}{D \sinh 2\pi d/L} \tag{28}$$

$$\text{Reynolds number} = \frac{u_{max}D}{\nu} = \frac{\pi HD \cosh\{2\pi(y+d)/L\}}{T\nu \sinh 2\pi d/L} \tag{29}$$

3.3 Wave-Induced Vibration of a Vertical Circular Cylinder

The natural frequencies of a circular cylinder as shown in Figure 13 are given by

$$f_i = \frac{a_i}{2\pi}\left[\frac{EI}{(m + m_w)\ell^3}\right]^{1/2} \tag{30}$$

where $I = \pi D^4/64$ is the moment of inertia, E is the Elastic Modulus, ℓ is the cylinder length, m is the mass of the cylinder, m_w is the added-mass of the water. Added-mass per unit length for a circular cross section is equal to $\rho\pi r^2$, where r is the radius of cylinder, and ρ is the mass density of water. Crede (1965) pointed out that the first three values of modal coefficient, a_i, are 3.52, 22.4 and 61.7.

The designer can adjust the values of E, I, and ℓ in order to make sure that the natural frequencies of the circular cylinder do not fall within the range of surface wave frequencies. A resonance condition may thus be avoided.

When waves pass a vertical circular cylinder, lateral vibration occurs due to vortex shedding. Under certain circumstances, this lateral vibration is not negligible. The destruction of the Texas Tower No. 4 off the coast of New Jersey (January 15, 1961) is attributed to coupling between the natural frequency of the structure and the vortex shedding frequency.

The non-dimensional Strouhal number S is used to define the vortex shedding frequency f_v which is a function of the cylinder diameter D and the maximum horizontal particle velocity u_{max}, where

$$S = \frac{f_v D}{u_{max}} \tag{31}$$

For circular cylinders, the empirical average value of the Strouhal number is about 0.2 for a sub-critical Reynolds number $Re \leq 2 \times 10^5$ (Ref. 28 ,Delany and Sorensen, 1953; Fung, 1960; Humphreys, 1960) in uniform rectilinear flow.

3.4 Froude's Model Laws

Froude's scaling laws are applied to hydraulic models when viscous and capillary effects are negligible. Froude's scaling system may be described as follows:

Length Scale: $\frac{\text{length of model}}{\text{length of prototype}} = n_L$

Time Scale: $n_t = n_L^{1/2}$

Velocity Scale: $n_v = n_L^{1/2}$

Mass Scale: $n_m = n_L^3$

Force Scale: $n_F = n_L^3$

Pressure Scale: $n_p = n_L$

Shearing Stress Scale: $n_\tau = n_L$

Drag Coefficient Scale: $n_{C_D} = 1$

Mass Coefficient Scale: $n_{C_M} = 1$

Elastic Modulus Scale: $n_E = n_L$

Poisson's Ratio Scale: $n_\mu = 1$

3.5 Experimental Technique

A rigid Poly Vinyl Chloride circular cylinder was used for all experiments. It had a length of 5 ft, 6 in. inside diameter and 9/32 in. wall thickness. The cylinder was attached to a 1 in. thick circular

aluminum base which was bolted to a 2 ft. diameter by 1/2 in. thick steel plate. This steel plate was anchor bolted to the bottom of the wave tank and a wooden annulus, ground board, was bolted to the steel plate.

Eight 120 Ω strain gauges were mounted vertically around the outside of the cylinder near the steel base, and were waterproofed as shown in Figure 15. The technique for measuring total moment and force was based on elastic beam theory. One Wheatstone bridge, made up of four active strain gauges to produce an output due to the tension or compression of the cylinder, was used to measure the longitudinal overturning moment about the base of the cylinder. Another Wheatstone bridge was used to measure the transverse overturning moment.

The cylinder was calibrated by applying loads to different points along the length of the cylinder. These loads varied from 2 lbs to 20 lbs, as shown in Figure 15 and Table 4. The calibration indicated a linear relationship between the loads applied and the strain readings. Therefore the values of strain obtained could be interpreted as the longitudinal or transverse moments about a reference height, S_1, (see Figure 13).

The centre of the cylinder was located at the centre line of the wave tank and 48 ft. from the static position of the wave generator. A wave gauge was located alongside the centre of the cylinder, midway between the cylinder and the tank wall to measure the wave heights, which were approximately the same as the incident wave heights measured without the cylinder in the wave tank, as shown in Figure 16.

Sinusoidal waves were generated in 3 ft. water depth throughout the tests. Four different wave periods 1.429 sec, 1.667 sec, 2 sec, and 2.5 sec were run and ten different wave heights were generated for each wave period. Data was recorded after the waves passing the cylinder reached a steady-state condition. A digital strain indicator (B and K type 1526) and a two-channel Hewlett-Packard 71003 strip chart recorder were used for this recording system, as shown in Figure 18.

The value of Elastic Modulus was found experimentally to be 5.073×10^5 psi. Figure 19 shows the tension specimen mounted in an Instron testing machine.

DISCUSSION OF RESULTS

The solid line represents theory in all graphs. The values of C_D, C_M, and C_L must be determined experimentally. When the crest (or trough) passes the center line of cylinder (zero acceleration), $2\pi(\frac{x}{L} - \frac{t}{T}) = 0^o$, C_D and C_L may be solved from equations (16) and (25). When the instantaneous water surface profile is at the still water level (zero velocity), $2\pi(\frac{x}{L} - \frac{t}{T}) = 90^o$, C_M may be solved from equation (16). Then the experimentally determined values of C_D, C_M, and C_L are used for computing theoretical moment and force. The action line of total resultant force to the cylinder may be calculated and a static calibration (TABLE 4) is utilized for computing the measured force.

The computer program based on linear wave theory which estimates the wave forces and overturning moments on the circular cylinder is given

in Appendix B. Values of C_D, C_M, and C_L may be obtained from this program. Results obtained from the program are given in Table 5.

The drag, mass, and lift coefficients are functions of Reynolds and Keulegan-Carpenter number (see Figures 20-25). When the ranges of Reynolds and Keulegan-Carpenter numbers are between 8.286×10^3 and 2.083×10^5 (subcritical regime), 0.6923 and 11.83, respectively, values of C_M and C_L vary between 0.675 to 1.22 and 0 to 0.17 respectively. C_M and C_L might be considered as constant for the wave periods 1.429 sec., 1.667 sec., and 2 sec. However, C_D varies from 0.307 to 7.418, as shown in Figures 20 and 21: In addition C_D is inversely related to H and u_{max}. That is, when the wave height becomes very small, C_D becomes very large, and u_{max} approaches zero. The wide variation of C_D has also been observed by a number of other investigators. Jan[12], and Pratte et al.[24] have presented data for the wave forces on a 6 in. diameter pile in 3 ft. water depth based on linear wave theory.

Values of C_D and C_M are shown in Table 5 to be independent of d/L, D/L, and d/T^2. Figures 26-29 show the maximum longitudinal and transverse forces versus Reynolds number and Keulegan-Carpenter number for four different wave periods. The longitudinal and transverse forces increase with increasing Re and $u_{max}T/D$. The transverse forces occur when the Keulegan-Carpenter number at the surface is greater than 5.27. Bidde[1] reported values of 3 to 5. Keulegan and Carpenter have observed a value of 15 for a horizontal rather than a vertical cylinder, using a standing wave with d/L being very small. When the Reynolds number is greater than 7.397×10^4, eddy shedding occurs.

Maximum forces and overturning moments are plotted as functions of wave steepness H/L for four different wave periods. The range of d/L is between 0.123 and 0.277, the range of H/L is between 0.003 and 0.105, and the range of D/L is between 0.023 and 0.051. Figures 30-33 show that the maximum forces and overturning moments are increasing functions of H/L. The theoretical and experimental results show reasonably good agreement. It should be noted that the maximum values of moment were taken as the mean value of all maxima observed.

Figure 17 shows symmetric vortex shedding behind the cylinder. The fundamental frequency of the cylinder is much higher than the wave frequency and the vortex-shedding frequency (equations (30) and (31)). Therefore, resonance does not occur.

4. CONCLUSIONS

The piston-type wave generator is capable of generating deep, intermediate and shallow water waves. A series of experiments have verified the ability of linear wave generator theory to predict wave motion associated with the stroke of the wave generator, wave height, water depth, and wave period. The theoretical and experimental results show better agreement for shallow water waves than intermediate water waves.

The measured wave forces and overturning moments on small diameter circular cylinder based on the linear wave theory show reasonably good agreement with theoretical results for the ranges of $0.123 < d/L < 0.277$, $0.003 < H/L < 0.105$, and $0.023 < D/L < 0.051$ in the wave periods of 1.429 sec., 1.667 sec., 2 sec., and 2.5 sec. The coefficients C_M and C_L have been found to have an overall average of 0.953 and 0.0535 respectively and might be considered as constants; while C_D was found to vary between 7.418 and 0.307 when the Reynolds number was in the range of 8.286×10^3 to 2.083×10^5 and the Keulegan-Carpenter number varied between 0.6923 and 11.83.

Transverse forces are related to vortex shedding. When the Keulegan-Carpenter number at the surface is greater than 5.27, transverse forces occur. Although the transverse forces and corresponding moments are small, they are not negligible when scaled up to prototype values (Froude's similitude requires that the force scale be equal to the third power of the length scale).

REFERENCES

1. Bidde, D.D., "Laboratory Study of Lift Forces on Circular Piles", Journal of the Waterways, Harbors and Coastal Engineering Division, Proceedings of the ASCE, WW4, November 1971.

2. Chakrabarti, S.K., "Wave Forces on Fixed Offshore Structure", ASCE National Structural Engineering Convention, New Orleans, Louisiana, April 14-18, 1975.

3. Chakrabarti, S.K., Tam, W.A., "Interaction of Waves with Large Vertical Cylinder", Journal of Ship Research, Vol. 19, No. 1, March 1975, pp. 23-33.

4. Hallermeier, R.J., "Nonlinear Flow of Wave Crests past a Thin Pile", Journal of the Waterways, Harbors and Coastal Engineering Division, WW4, November, 1976.

5. Hansen, J.B., Schiolten, P., Svendsen, I.A., "Laboratory Generation of Waves of Constant Form", Institute of Hydrodynamics and Hydraulic Engineering Technical University of Denmark, November 1975.

6. Hogben, N., "Wave Loads on Structures", Ship Division, National Physical Laboratory, England, BOSS '76.

7. Hogben, N., Miller, B.L., Searle, J.W., Ward, G., "Estimation of Fluid Loading on Offshore Structure", Proc. Instn. Civ. Engrs., Part 2, 63, September 1977, pp. 515-562.

8. Ippen, "Estuary and Coastline Hydrodynamics", McGraw-Hill Book Company, 1966.

9. Isaacson, M. de St. Q., "Shallow Wave Diffraction Around Large Cylinder", Journal of the Water, Port, Coastal and Ocean Division, WW1, February 1977.

10. Isaacson, M. de St. Q., Maull, D.J., "Transverse Forces on Vertical Cylinders in Waves", Journal of the Waterways, Harbors and Coastal Engineering Division, WW1, February 1976.

11. Isaacson, M. de St. Q., "Nonlinear Wave Forces on Large Offshore Structures", Journal of the Waterway, Port, Coastal and Ocean Division, Technical Notes, February 1977.

12. Jen, Y., "Wave Forces on Circular Cylindrical Piles Used in Coastal Structures", University of California, Berkeley, Hydraulic Engineering Laboratory, Technical Report HEL 9-11, January 1967, 98 pp.

13. Keating, T., Webber, N.B., "The Generation of Periodic Waves in a Laboratory Channel: A Comparison Between Theory and Experiment", Proc. Instn. Civ. Engrs., Part 2, 63, December 1966, pp. 819-832.

14. King, R., "Vortex Excited Structural Oscillations of a Circular Cylinder in Steady Current", Offshore Technology Conference, Dallas, 1974.

15. Kolkman, P.A., Weide, J. Van Der, "Elastic Similarity Models as a Tool for Offshore Engineering Development", Delft. Hydraulics Laboratory, Publication No. 99, April 1972.

16. Le Méhauté, B., "Similitude in Coastal Engineering", Journal of the Waterways, Harbors, and Coastal Engineering Division, ww3, August 1976.

17. Le Méhauté, B., "An Introduction to Hydrodynamics and Water Waves", Springer - Verlag Book Company, 1976.

18. MacCamy, R.C., Fuchs, R.A., "Wave Forces on Piles: A Diffraction Theory", U.S. Army, Corps. of Engineering, Beach Erosion Board, Technical Memorandum, No. 69, December 1954, 17 pp.

19. McCormick, M.E., "Ocean Engineering Wave Mechanics", A Wiley - Interscience Publication, 1973.

20. Mogridge, G.R., Jamieson, W.W., "Wave Loads on Large Circular Cylinders: A Design Method", Hydraulics Laboratory, NRC, Ottawa.

21. Morison, J.R., O'Brien, M.P., Johnson, J.W., Schaaf, S.A., "The Force Exerted by Surface Waves on Piles", Petroleum Transactions, AIME, Vol. 189, 1950, pp. 149-154.

22. Morison, J.R., Johnson, J.W., O'Brien, M.P., "Experimental Studies of Forces on Piles", Proceedings, 4th Conference on Coastal Engineering, Council on Wave Research, Berkeley, Calif., 1954, pp. 340-370.

23. Perry and Lissner, "The Strain Gage Primer", Second Edition, McGraw-Hill Book Company, 1962.

24. Pratte, B.D., Funke, E.R., Mogridge, G.R., Jamieson, W.W., "Wave Forces on a Model Pile", Proc. First Canadian Hydraulics Conf., Edmonton, 1973, pp. 523-543.

25. Raman, H., Venkatanarasaiah, P., "Forces due to Nonlinear Waves on Vertical Cylinders", Proc. ASCE, Vol. 102, No. WW3, August 1976, pp. 301-316.

26. Smith, A.A., "Laboratory Wave Generation: A Comparison of Theoretical and Experimental Performance", The Royal College of Science and Technology, Glasgow, Scotland, I.A.H.R. Congress, London, 1963.

27. Ursell, F., Dean, R.G., Yu, Y.S., "Forced Small-Amplitude Water Waves: A Comparison of Theory and Experiment", J. Fluid Mech., 7, 1960, pp. 33-52.

28. Wiegel, R.L., "Oceanographical Engineering", Prentice-Hall, Inc., Englewood Cliffs, N.Y., 1964.

29. Wiegel, R.L., Beebe, K.E., Moon, J., "Ocean-Wave Forces on Circular Cylindrical Piles", J. Hyd. Div., A.S.C.E., 83, HY2, paper 1199, April 1957, pp. 1-36.

30. Wootton, L.R., Warner, M.H., Cooper, D.H., "Some Aspects of the Oscillations of Full-Scale Piles", National Physical Laboratory, England.

TABLE 1

Calibration Results: Wave Parameters for 4.5 ft Water Depth

f(Hz)	Span(%)	e(in.)	H(ft)	L(ft)	d/L	H/L	2πd/L	H/e
0.2	10	0.94	0.07	59.5	0.076	0.0012	0.49	0.90
0.2	20	1.88	0.16	60.0	0.075	0.0027	0.49	1.03
0.2	30	2.88	0.31	56.9	0.079	0.0055	0.49	1.29
0.2	40	3.88	0.34	56.0	0.080	0.0061	0.49	1.05
0.2	50	4.88	0.39	55.8	0.080	0.0070	0.49	0.96
0.2	60	5.88	0.56	56.5	0.080	0.0099	0.49	1.14
0.2	70	6.75	0.56	60.7	0.074	0.0092	0.49	1.00
0.2	80	7.63	0.64	56.0	0.080	0.0110	0.49	1.00
0.2	90	8.69	0.75	56.7	0.079	0.0130	0.49	1.53
0.3	10	0.78	0.10	36.69	0.123	0.0027	0.72	1.54
0.3	20	1.59	0.19	37.26	0.121	0.0051	0.72	1.43
0.3	30	2.44	0.23	41.25	0.109	0.0056	0.72	1.13
0.3	40	3.28	0.22	38.50	0.117	0.0057	0.72	1.54
0.3	50	4.13	0.56	39.75	0.113	0.0141	0.72	1.63
0.3	60	4.88	0.70	39.10	0.115	0.0179	0.72	1.75
0.3	70	5.56	0.81	41.25	0.109	0.0196	0.72	1.76
0.3	80	6.41	0.81	41.25	0.109	0.0196	0.72	1.53
0.3	90	7.59	1.01	38.50	0.117	0.0262	0.72	2.53
0.4	10	0.63	0.22	25.74	0.175	0.0085	1.10	4.23
0.4	20	1.34	0.23	25.74	0.175	0.0089	1.10	2.05
0.4	30	2.06	0.34	25.74	0.175	0.0132	1.10	1.98
0.4	40	2.75	0.47	25.74	0.175	0.0183	1.10	2.05
0.4	50	3.06	0.59	25.74	0.175	0.0229	1.10	2.02
0.4	60	4.09	0.68	25.74	0.175	0.0264	1.10	2.00
0.4	70	5.56	0.80	25.74	0.175	0.0311	1.10	1.74
0.4	80	5.38	0.96	25.74	0.175	0.0373	1.10	2.13

TABLE 1-Continued

f(Hz)	Span(%)	e(in.)	H(ft)	L(ft)	d/L	H/L	2πd/L	H/e
0.5	10	0.53	0.13	19.18	0.2346	0.0068	1.43	2.95
0.5	20	1.13	0.31	19.66	0.2289	0.0158	1.43	3.33
0.5	30	1.75	0.47	19.86	0.2266	0.0237	1.43	2.73
0.5	40	2.38	0.65	20.00	0.2250	0.0325	1.43	3.28
0.5	50	2.56	0.71	20.00	0.2250	0.0355	1.43	3.32
0.5	60	3.53	0.94	20.58	0.2186	0.0457	1.43	3.24
0.5	70	4.09	1.07	19.44	0.2315	0.0550	1.43	3.15
0.5	80	4.63	1.19	19.93	0.2258	0.0597	1.43	3.05
0.5	90	5.06	1.28	20.00	0.2250	0.0640	1.43	4.44
0.6	10	0.89	0.13	15.31	0.2939	0.0085	1.89	3.61
0.6	20	0.97	0.33	14.69	0.3063	0.0225	1.89	3.83
0.6	30	1.53	0.47	14.50	0.3103	0.0324	1.89	3.67
0.6	40	2.06	0.61	14.89	0.3022	0.0410	1.89	3.55
0.6	50	2.25	0.72	14.89	0.3022	0.0484	1.89	3.83
0.6	60	3.03	0.87	14.89	0.3022	0.0584	1.89	3.48
0.6	70	3.59	0.94	14.88	0.3022	0.0632	1.89	3.13
0.6	80	4.03	1.02	15.00	0.3000	0.0680	1.89	3.00
0.7	10	0.81	0.17	11.03	0.4080	0.0154	2.50	5.00
0.7	20	0.84	0.34	11.03	0.4080	0.0308	2.50	4.86
0.7	30	1.34	0.50	10.89	0.4132	0.0459	2.50	4.46
0.7	40	1.81	0.59	11.88	0.3788	0.0497	2.50	4.37
0.7	50	2.03	0.74	11.14	0.4039	0.0664	2.50	4.38
0.7	60	2.72	0.82	11.14	0.4039	0.0736	2.50	3.57
0.7	70	3.19	0.96	11.53	0.3903	0.0833	2.50	3.56
0.7	80	3.59	0.99	11.53	0.3903	0.0859	2.50	3.30

TABLE 1-Continued

f(Hz)	Span(%)	e(in.)	H(ft)	L(ft)	d/L	H/L	2πd/L	H/e
0.8	10	0.34	0.15	8.57	0.5251	0.0175	3.30	5.17
0.8	20	0.72	0.47	8.27	0.5441	0.0568	3.30	7.83
0.8	30	1.18	0.55	8.17	0.5508	0.0673	3.30	5.56
0.8	40	1.63	0.60	7.96	0.5653	0.0754	3.30	4.44
0.8	50	1.81	0.69	8.93	0.5039	0.0773	3.30	4.64
0.8	60	2.44	0.79	9.02	0.4989	0.0876	3.30	3.95
0.9	10	0.36	0.12	6.45	0.6977	0.0186	4.21	4.61
0.9	20	0.60	0.24	6.49	0.6934	0.0370	4.21	4.53
0.9	30	1.08	0.35	6.50	0.6923	0.0538	4.21	3.85
0.9	40	1.44	0.52	6.88	0.6541	0.0756	4.21	4.26
0.9	50	1.68	0.58	7.07	0.6365	0.0820	4.21	4.30

TABLE 2

Calibration Results: Wave Parameters for 3 ft Water Depth

f(Hz)	Span(%)	e(in.)	H(ft)	L(ft)	d/L	H/L	2πd/L	H/e
0.2	10	0.97	0.06	50.00	0.060	0.0012	0.38	0.75
0.2	20	2.00	0.13	50.72	0.059	0.0026	0.38	0.76
0.2	30	3.00	0.18	51.47	0.058	0.0035	0.38	0.72
0.2	40	4.03	0.27	50.00	0.060	0.0054	0.38	0.79
0.2	50	5.09	0.34	50.72	0.059	0.0067	0.38	0.81
0.2	60	6.13	0.41	51.47	0.058	0.0080	0.38	0.80
0.2	70	7.13	0.49	50.00	0.060	0.0098	0.38	0.83
0.2	80	8.16	0.56	50.00	0.060	0.0112	0.38	0.82
0.2	90	9.06	0.67	50.72	0.059	0.0132	0.38	0.88
0.2	100	10.00	0.74	50.70	0.059	0.0146	0.38	0.89
0.3	10	0.78	0.085	33.06	0.09	0.0026	0.57	1.29
0.3	20	1.75	0.19	33.03	0.09	0.0058	0.57	1.27
0.3	30	2.63	0.27	33.50	0.09	0.0080	0.57	1.23
0.3	40	3.53	0.37	33.03	0.09	0.0110	0.57	1.28
0.3	50	4.38	0.47	33.50	0.09	0.0140	0.57	1.31
0.3	60	5.25	0.56	32.53	0.09	0.0170	0.57	1.27
0.3	70	6.09	0.67	33.00	0.09	0.0200	0.57	1.31
0.3	80	6.97	0.74	33.03	0.09	0.0220	0.57	1.28
0.3	90	7.81	0.82	33.50	0.09	0.0240	0.57	1.26
0.3	100	8.63	0.91	33.50	0.09	0.0270	0.57	1.26
0.4	10	0.68	0.08	23.33	0.1286	0.0034	0.80	1.33
0.4	20	1.44	0.21	23.33	0.1286	0.0090	0.80	1.91
0.4	30	2.25	0.34	23.65	0.1286	0.0144	0.80	1.79
0.4	40	3.06	0.48	23.03	0.1300	0.0208	0.80	1.85
0.4	50	3.81	0.58	24.30	0.1235	0.0239	0.80	1.81
0.4	60	4.53	0.68	23.03	0.1300	0.0295	0.80	1.79
0.4	70	5.25	0.80	22.73	0.1320	0.0352	0.80	1.82
0.4	80	5.97	0.89	23.65	0.1268	0.0376	0.80	1.78
0.4	90	6.66	0.98	24.31	0.1234	0.0400	0.80	1.78
0.4	100	7.31	1.06	24.31	0.1234	0.0436	0.80	1.74

TABLE 2-Continued

f(Hz)	Span(%)	e(in.)	H(ft)	L(ft)	d/L	H/L	2πd/L	H/e
0.5	10	0.59	0.12	17.72	0.169	0.0068	1.05	2.40
0.5	20	1.75	0.27	18.18	0.165	0.0149	1.05	1.80
0.5	30	1.94	0.42	17.95	0.167	0.0234	1.05	2.62
0.5	40	2.63	0.54	20.00	0.150	0.0270	1.05	2.45
0.5	50	3.28	0.69	17.95	0.167	0.0384	1.05	2.56
0.5	60	3.86	0.80	17.72	0.169	0.0450	1.05	2.50
0.5	70	4.53	0.92	17.95	0.167	0.0510	1.05	2.42
0.5	80	5.09	1.00	18.18	0.165	0.0550	1.05	2.38
0.5	90	5.69	1.14	17.95	0.167	0.0635	1.05	2.43
0.5	100	6.31	1.33	17.95	0.167	0.0740	1.05	2.51
0.6	10	0.50	0.13	13.13	0.2285	0.0099	1.41	3.25
0.6	20	1.06	0.28	13.43	0.2234	0.0210	1.41	3.11
0.6	30	1.69	0.45	13.68	0.2193	0.0329	1.41	3.21
0.6	40	2.31	0.58	13.58	0.2210	0.0427	1.41	3.05
0.6	50	2.88	0.74	13.13	0.2285	0.0560	1.41	3.08
0.6	60	3.38	0.85	13.18	0.2285	0.0650	1.41	3.04
0.6	70	3.88	0.96	13.58	0.2210	0.0700	1.41	3.00
0.6	80	4.44	1.20	13.18	0.2285	0.0910	1.41	3.24
0.6	90	4.94	1.27	13.35	0.2247	0.0948	1.41	3.08
0.6	100	5.50	1.34	13.35	0.2247	0.1006	1.41	2.93
0.7	10	0.47	0.14	10.82	0.277	0.0129	1.70	3.50
0.7	20	0.94	0.30	11.07	0.271	0.0271	1.70	3.75
0.7	30	1.50	0.44	11.05	0.271	0.0398	1.70	3.38
0.7	40	2.00	0.58	10.94	0.274	0.0530	1.70	3.41
0.7	50	2.50	0.71	10.94	0.274	0.0649	1.70	3.38
0.7	60	3.00	0.82	11.41	0.263	0.0719	1.70	3.28
0.7	70	3.50	0.90	11.67	0.257	0.0770	1.70	3.10
0.7	80	4.00	1.02	11.08	0.271	0.0920	1.70	3.06
0.7	90	4.38	1.09	11.08	0.271	0.0980	1.70	2.99
0.7	100	4.81	1.16	11.08	0.271	0.1050	1.70	2.89

TABLE 2-Continued

f(Hz)	Span(%)	e(in.)	H(ft)	L(ft)	d/L	H/L	2πd/L	H/e
0.8	10	0.41	0.14	8.33	0.360	0.017	2.18	4.67
0.8	20	0.88	0.30	8.33	0.360	0.036	2.18	4.29
0.8	30	1.31	0.42	8.67	0.346	0.048	2.18	3.82
0.8	40	1.81	0.55	8.75	0.343	0.063	2.18	3.67
0.8	50	2.25	0.64	9.10	0.330	0.070	2.18	3.37
0.8	60	2.69	0.74	8.75	0.343	0.085	2.18	3.36
0.9	10	0.37	0.13	6.53	0.4594	0.020	2.81	4.33
0.9	20	0.75	0.28	6.28	0.4778	0.045	2.81	4.67
0.9	30	1.22	0.42	6.53	0.4594	0.064	2.81	4.20
0.9	40	1.63	0.50	7.32	0.4098	0.068	2.81	3.57
0.9	50	2.06	0.64	7.32	0.4098	0.087	2.81	3.76
1.0	10	0.31	0.13	6.36	0.472	0.020	3.45	4.33
1.0	20	0.69	0.25	5.47	0.548	0.046	3.45	4.17
1.0	30	1.06	0.38	5.47	0.548	0.069	3.45	4.22
1.0	40	1.47	0.48	5.60	0.536	0.086	3.45	4.00

TABLE 3

Attenuation Coefficients

f(Hz)	d(ft)	H_1(ft)	H_2(ft)	L(ft)	$K_{mea.}$ (ft^{-1})=$\ln(H_1/H_2)/61.8ft$	$K_{theo.}$ (ft^{-1})
0.4	3	1.031	1.0267	22.070	6.763×10^{-5}	8.487×10^{-5}
0.4	3	1.187	1.1846	23.804	3.275×10^{-5}	7.973×10^{-5}
0.4	3	0.942	0.9390	23.804	4.302×10^{-5}	7.973×10^{-5}
0.5	3	0.731	0.7298	18.025	3.544×10^{-5}	8.889×10^{-5}
0.5	3	0.850	0.8470	17.050	5.720×10^{-5}	9.258×10^{-5}
0.5	3	0.990	0.9854	18.847	7.536×10^{-5}	8.596×10^{-5}
0.6	3	0.798	0.7940	13.510	8.131×10^{-5}	9.882×10^{-5}
0.6	3	0.924	0.9190	13.730	8.780×10^{-5}	9.782×10^{-5}

TABLE 4

Model Calibration

Location of Load(ft)	Load(lb)									
	2	4	6	8	10	12	14	16	18	20
2.500	12	24	36	49	62	74	86	99	110	123
2.333	12	23	35	46	57	68	80	91	102	114
2.167	10	21	31	42	52	63	73	84	95	105
2.000	10	20	30	39	49	59	68	78	88	98
1.917	10	19	29	38	48	57	66	76	85	94
1.833	9	18	27	36	45	54	63	72	81	90
1.750	8	17	26	34	43	52	60	69	77	86
1.667	8	16	24	33	41	49	58	66	73	82
1.583	8	16	24	32	39	47	55	63	70	78
1.500	7	15	22	30	37	45	52	59	67	74
1.417	7	14	21	28	35	42	49	55	63	70
1.333	7	13	20	27	33	40	47	53	60	66
1.250	6	12	18	24	30	36	42	49	55	61
1.000	4	9	14	19	24	29	34	39	44	49

Inset values are strains($\times 10^{-6}$).

Location of load is based on a datum level of 0 ft at the wave tank floor.

TABLE 5

Measured Wave Forces and Moments

Run	f(Hz)	H(ft)	L(ft)	d/L	H/L	D/L	df^2	u_{max} (ft/sec)
1	0.4	0.080	23.330	0.129	0.003	0.023	0.480	0.1515E 00
2	0.4	0.210	23.330	0.129	0.009	0.023	0.480	0.4024E 00
3	0.4	0.340	23.650	0.127	0.014	0.023	0.480	0.6505E 00
4	0.4	0.480	23.030	0.130	0.021	0.024	0.480	0.9361E 00
5	0.4	0.590	24.300	0.123	0.024	0.023	0.480	0.1179E 01
6	0.4	0.680	23.030	0.130	0.030	0.024	0.480	0.1352E 01
7	0.4	0.800	22.730	0.132	0.035	0.024	0.480	0.1599E 01
8	0.4	0.930	23.650	0.127	0.038	0.023	0.480	0.1833E 01
9	0.4	0.990	24.310	0.123	0.040	0.023	0.480	0.2066E 01
10	0.4	1.060	24.310	0.123	0.044	0.023	0.480	0.2251E 01
11	0.5	0.120	17.720	0.169	0.007	0.031	0.750	0.2435E 00
12	0.5	0.270	18.180	0.165	0.015	0.030	0.750	0.5565E 00
13	0.5	0.420	17.950	0.167	0.023	0.030	0.750	0.8946E 00
14	0.5	0.540	20.000	0.150	0.027	0.027	0.750	0.1228E 01
15	0.5	0.690	17.950	0.167	0.038	0.030	0.750	0.1528E 01
16	0.5	0.800	17.720	0.169	0.045	0.031	0.750	0.1791E 01
17	0.5	0.920	17.950	0.167	0.051	0.030	0.750	0.2106E 01
18	0.5	1.000	18.180	0.165	0.055	0.030	0.750	0.2326E 01
19	0.5	1.140	17.950	0.167	0.064	0.030	0.750	0.2696E 01
20	0.5	1.330	17.950	0.167	0.074	0.030	0.750	0.3236E 01
21	0.6	0.130	13.130	0.228	0.010	0.042	1.080	0.2822E 00
22	0.6	0.250	13.430	0.223	0.021	0.041	1.080	0.6315E 00
23	0.6	0.450	13.680	0.219	0.033	0.040	1.080	0.1056E 01
24	0.6	0.580	13.580	0.221	0.043	0.040	1.080	0.1397E 01
25	0.6	0.740	13.130	0.228	0.056	0.042	1.080	0.1835E 01
26	0.6	0.850	13.180	0.228	0.064	0.042	1.080	0.2161E 01
27	0.6	0.960	13.580	0.221	0.071	0.040	1.080	0.2506E 01
28	0.6	1.200	13.180	0.228	0.091	0.042	1.080	0.3297E 01
29	0.6	1.266	13.350	0.225	0.095	0.041	1.080	0.3529E 01
30	0.6	1.343	13.350	0.225	0.101	0.041	1.080	0.3808E 01
31	0.7	0.140	10.820	0.277	0.013	0.051	1.470	0.3402E 00
32	0.7	0.300	11.070	0.271	0.027	0.049	1.470	0.7538E 00
33	0.7	0.440	11.050	0.271	0.040	0.050	1.470	0.1163E 01
34	0.7	0.580	10.940	0.274	0.053	0.050	1.470	0.1592E 01
35	0.7	0.710	10.940	0.274	0.065	0.050	1.470	0.2019E 01
36	0.7	0.820	11.410	0.263	0.072	0.048	1.470	0.2401E 01
37	0.7	0.900	11.670	0.257	0.077	0.047	1.470	0.2590E 01
38	0.7	1.020	11.080	0.271	0.092	0.049	1.470	0.3156E 01
39	0.7	1.090	11.080	0.271	0.098	0.049	1.470	0.3438E 01
40	0.7	1.160	11.080	0.271	0.105	0.049	1.470	0.3730E 01

Run	u_{max} T/D	Re	MM_{S_1} (lb-ft)	C_D	C_H
1	0.6923E 00	0.8266E 04	0.706	7.418	1.144
2	0.1839E 01	0.2201E 05	1.765	2.282	1.003
3	0.3039E 01	0.3636E 05	3.531	1.470	1.115
4	0.4278E 01	0.5120E 05	5.297	1.086	1.111
5	0.5387E 01	0.6448E 05	7.416	0.746	1.098
6	0.6180E 01	0.7397E 05	9.535	0.973	1.220
7	0.7306E 01	0.8745E 05	12.360	0.882	1.175
8	0.8377E 01	0.1003E 06	15.185	1.274	1.151
9	0.9443E 01	0.1130E 06	18.010	1.228	1.174
10	0.1029E 02	0.1232E 06	20.129	1.208	1.048
11	0.8905E 00	0.1332E 05	1.059	5.284	0.912
12	0.2071E 01	0.3099E 05	2.825	3.390	0.992
13	0.3271E 01	0.4894E 05	4.591	0.510	0.884
14	0.4490E 01	0.6718E 05	7.063	0.995	1.014
15	0.5585E 01	0.8356E 05	9.535	1.110	0.943
16	0.6550E 01	0.9799E 05	11.654	0.982	0.937
17	0.7700E 01	0.1152E 06	13.066	0.921	0.842
18	0.8503E 01	0.1272E 06	15.538	0.637	1.026
19	0.9856E 01	0.1475E 06	17.657	0.581	0.873
20	0.1183E 02	0.1770E 06	21.189	0.604	0.755
21	0.8599E 00	0.1544E 05	1.059	3.924	0.735
22	0.1924E 01	0.3454E 05	3.178	3.195	0.936
23	0.3219E 01	0.5778E 05	6.003	2.003	1.002
24	0.4256E 01	0.7641E 05	9.182	1.416	1.125
25	0.5592E 01	0.1004E 06	11.654	1.012	0.997
26	0.6583E 01	0.1182E 06	13.420	0.767	0.956
27	0.7635E 01	0.1371E 06	16.598	0.818	0.879
28	0.1005E 02	0.1803E 06	19.423	0.507	0.802
29	0.1075E 02	0.1931E 06	21.189	0.753	0.675
30	0.1162E 02	0.2083E 06	23.308	0.670	0.709
31	0.8884E 00	0.1861E 05	1.413	3.738	0.762
32	0.1995E 01	0.4178E 05	4.239	1.238	0.933
33	0.3038E 01	0.6362E 05	8.122	0.307	1.149
34	0.4157E 01	0.8707E 05	10.594	0.594	1.087
35	0.5274E 01	0.1105E 06	12.713	0.375	0.958
36	0.6271E 01	0.1313E 06	14.832	0.381	0.910
37	0.7024E 01	0.1471E 06	15.892	0.522	0.778
38	0.8243E 01	0.1727E 06	19.423	0.488	0.803
39	0.8979E 01	0.1881E 06	21.189	0.456	0.740
40	0.9741E 01	0.2040E 06	22.248	0.531	0.780

Run	β_{hm}	β_{hf}	M_{S_1} (lb-ft)	F_h (lb)	MF_h (lb)	L1 (ft)
1	90.000	90.000	0.706	0.478	0.571	1.478
2	90.000	90.000	1.713	1.131	1.429	1.515
3	90.000	90.000	3.286	2.119	2.500	1.550
4	90.000	90.000	4.767	2.989	3.750	1.595
5	90.000	90.000	6.194	3.835	5.250	1.615
6	90.000	90.000	8.009	4.945	6.750	1.653
7	90.000	90.000	9.394	5.655	8.485	1.691
8	38.765	41.199	12.201	6.960	10.000	1.753
9	35.496	37.074	14.931	8.392	11.547	1.779
10	29.002	30.955	16.409	9.026	12.670	1.818
11	90.000	90.000	1.059	0.689	0.750	1.537
12	57.336	66.343	2.864	1.793	2.000	1.593
13	90.000	90.000	4.132	2.539	3.250	1.627
14	90.000	90.000	6.971	4.253	5.000	1.639
15	69.017	90.000	8.124	4.735	6.480	1.716
16	64.445	81.249	9.724	5.528	7.765	1.759
17	47.422	53.826	11.083	6.067	8.220	1.827
18	90.000	90.000	14.606	8.086	10.000	1.806
19	72.658	90.000	14.848	7.995	11.111	1.857
20	41.810	47.435	17.445	8.799	12.200	1.983
21	90.000	90.000	1.050	0.653	0.750	1.622
22	89.355	90.000	3.178	1.908	2.250	1.666
23	90.000	90.000	6.003	3.496	4.000	1.717
24	90.000	90.000	9.182	5.203	6.000	1.765
25	90.000	90.000	10.947	5.968	7.333	1.834
26	90.000	90.000	12.713	6.792	8.216	1.872
27	72.247	90.000	14.143	7.442	9.792	1.900
28	90.000	90.000	17.657	8.838	11.166	1.998
29	35.100	41.311	18.796	8.764	11.430	2.145
30	36.120	46.498	20.737	9.633	12.570	2.152
31	90.000	90.000	1.413	0.832	1.000	1.698
32	90.000	90.000	4.096	2.345	2.823	1.747
33	90.000	90.000	7.946	4.415	5.111	1.800
34	90.000	90.000	10.594	5.706	6.667	1.857
35	90.000	90.000	12.219	6.410	7.579	1.906
36	90.000	90.000	14.479	7.514	8.750	1.927
37	90.000	90.000	14.302	7.750	9.375	1.946
38	90.000	90.000	17.304	8.574	11.186	2.018
39	90.000	90.000	17.657	8.633	12.203	2.045
40	90.000	90.000	20.482	9.883	12.368	2.072

Run	MM_{ST}(lb-ft)	C_L	F_T(lb)	MF_T(lb)	M_{ST}(lb-ft)	L2(ft)
1	0.000	0.000	0.000	0.000	0.000	0.000
2	0.000	0.000	0.000	0.000	0.000	0.000
3	0.000	0.000	0.000	0.000	0.000	0.000
4	0.000	0.000	0.000	0.000	0.000	0.000
5	0.000	0.000	0.000	0.000	0.000	0.000
6	0.353	0.036	0.073	0.215	0.127	1.754
7	1.413	0.101	0.283	0.886	0.509	1.799
8	1.413	0.119	0.452	0.886	0.819	1.815
9	1.766	0.120	0.597	1.111	1.095	1.834
10	2.625	0.170	1.002	1.768	1.865	1.861
11	0.000	0.000	0.000	0.000	0.000	0.000
12	0.000	0.000	0.000	0.000	0.000	0.000
13	0.000	0.000	0.000	0.000	0.000	0.000
14	0.000	0.000	0.000	0.000	0.000	0.000
15	0.353	0.042	0.087	0.200	0.162	1.868
16	0.353	0.030	0.085	0.200	0.162	1.917
17	0.706	0.050	0.199	0.361	0.338	1.956
18	1.059	0.043	0.214	0.540	0.424	1.980
19	1.766	0.059	0.380	0.905	0.777	2.042
20	2.119	0.060	0.570	1.091	1.208	2.118
21	0.000	0.000	0.000	0.000	0.000	0.000
22	0.000	0.000	0.000	0.000	0.000	0.000
23	0.000	0.000	0.000	0.000	0.000	0.000
24	0.000	0.000	0.000	0.000	0.000	0.000
25	0.000	0.000	0.000	0.000	0.000	0.000
26	0.353	0.021	0.063	0.178	0.134	2.136
27	0.706	0.034	0.144	0.358	0.311	2.162
28	1.413	0.037	0.259	0.615	0.593	2.295
29	1.766	0.062	0.504	0.769	1.165	2.314
30	2.119	0.060	0.568	0.923	1.335	2.349
31	0.000	0.000	0.000	0.000	0.000	0.000
32	0.000	0.000	0.000	0.000	0.000	0.000
33	0.000	0.000	0.000	0.000	0.000	0.000
34	0.000	0.000	0.000	0.000	0.000	0.000
35	0.353	0.010	0.022	0.167	0.049	2.217
36	0.353	0.009	0.028	0.167	0.064	2.236
37	0.706	0.022	0.091	0.333	0.205	2.255
38	1.059	0.027	0.139	0.461	0.328	2.356
39	1.059	0.023	0.142	0.461	0.339	2.389
40	1.766	0.042	0.306	0.769	0.742	2.423

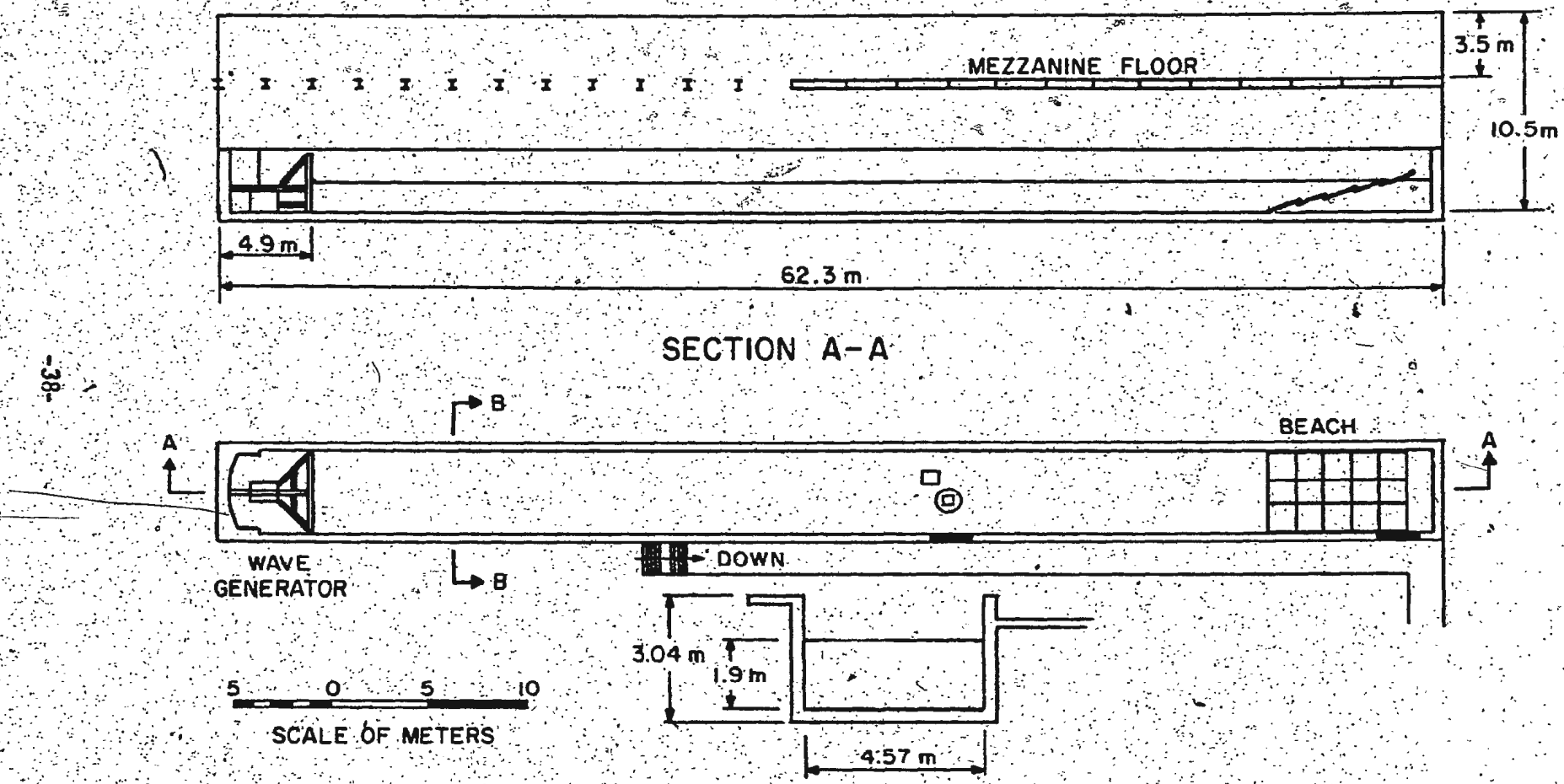

Fig. 1: Elevation and Plan Views of Wave Tank

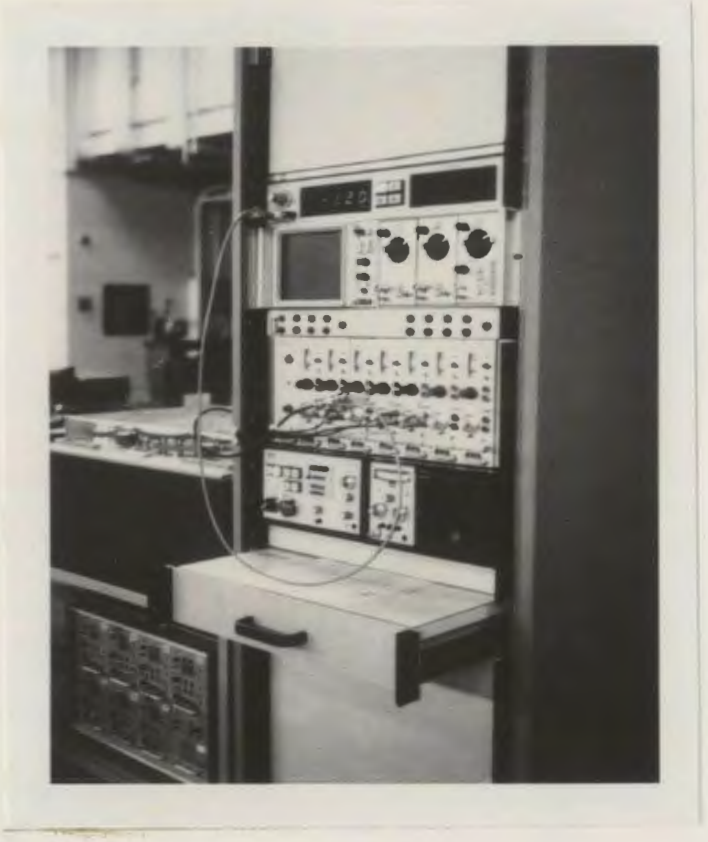

Fig. 2: Wave Generator Control Console

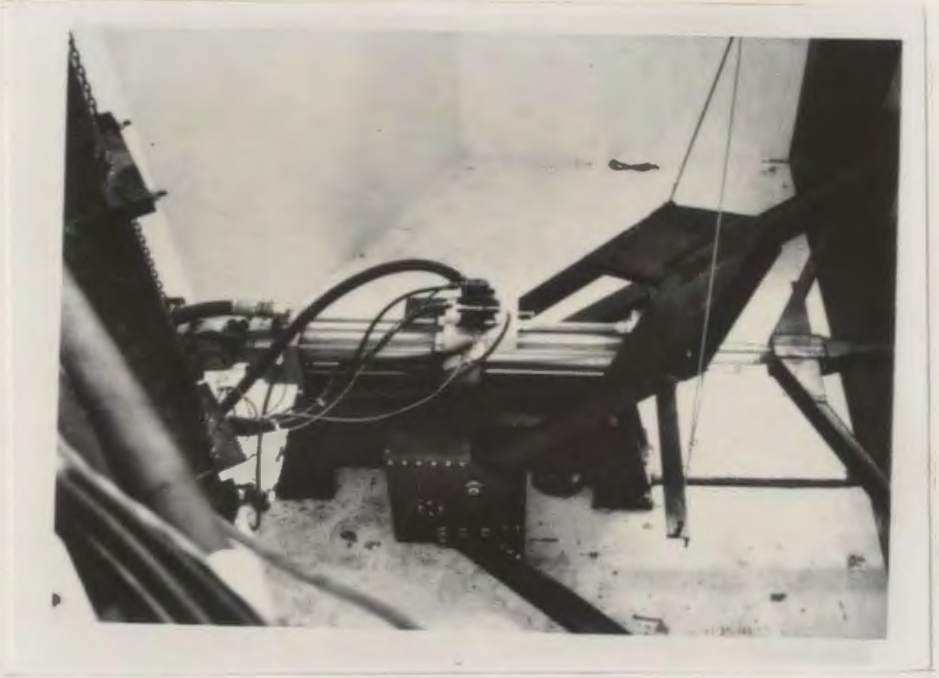

Fig. 3: Hydraulic Actuator

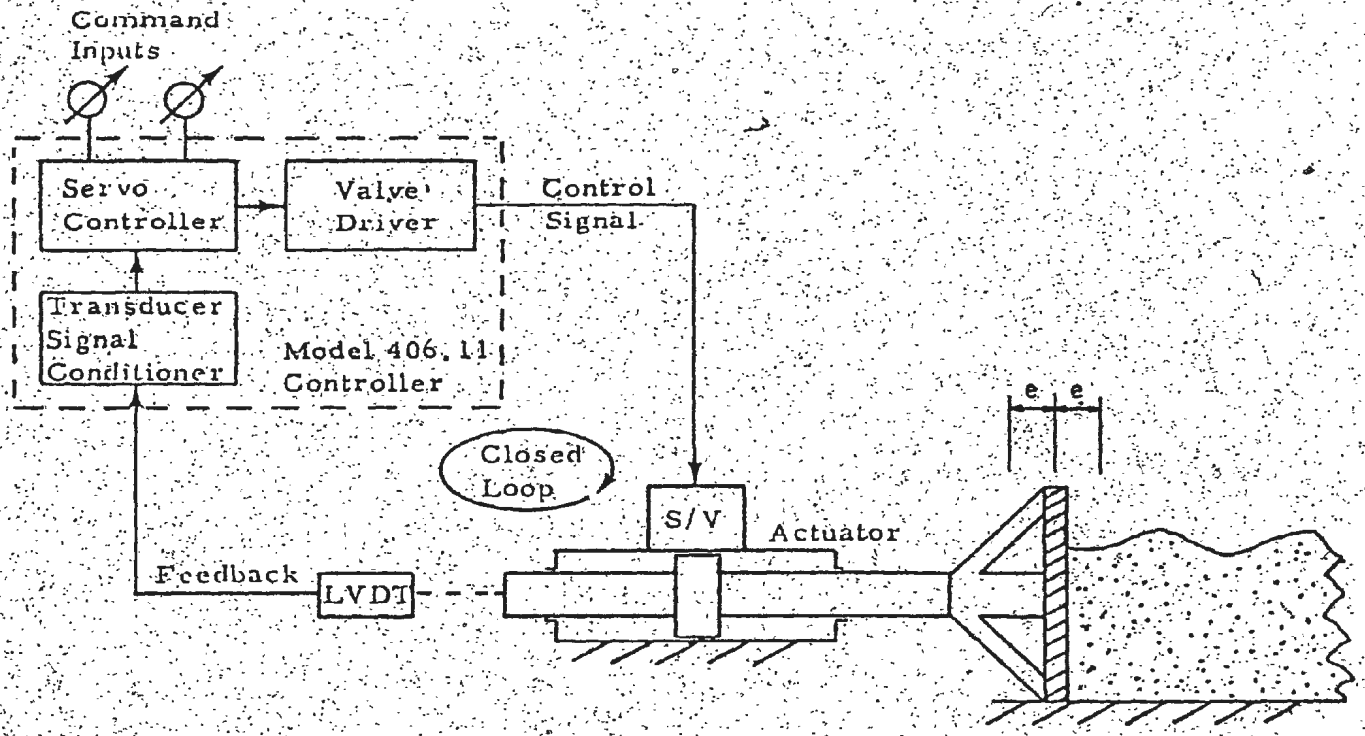

Fig. 4: Control Loop for Piston-Type Wave Generator

Fig. 5: Wave Absorbing Beach (Slope 1:6.2)

Fig. 6: General View of Wave Tank

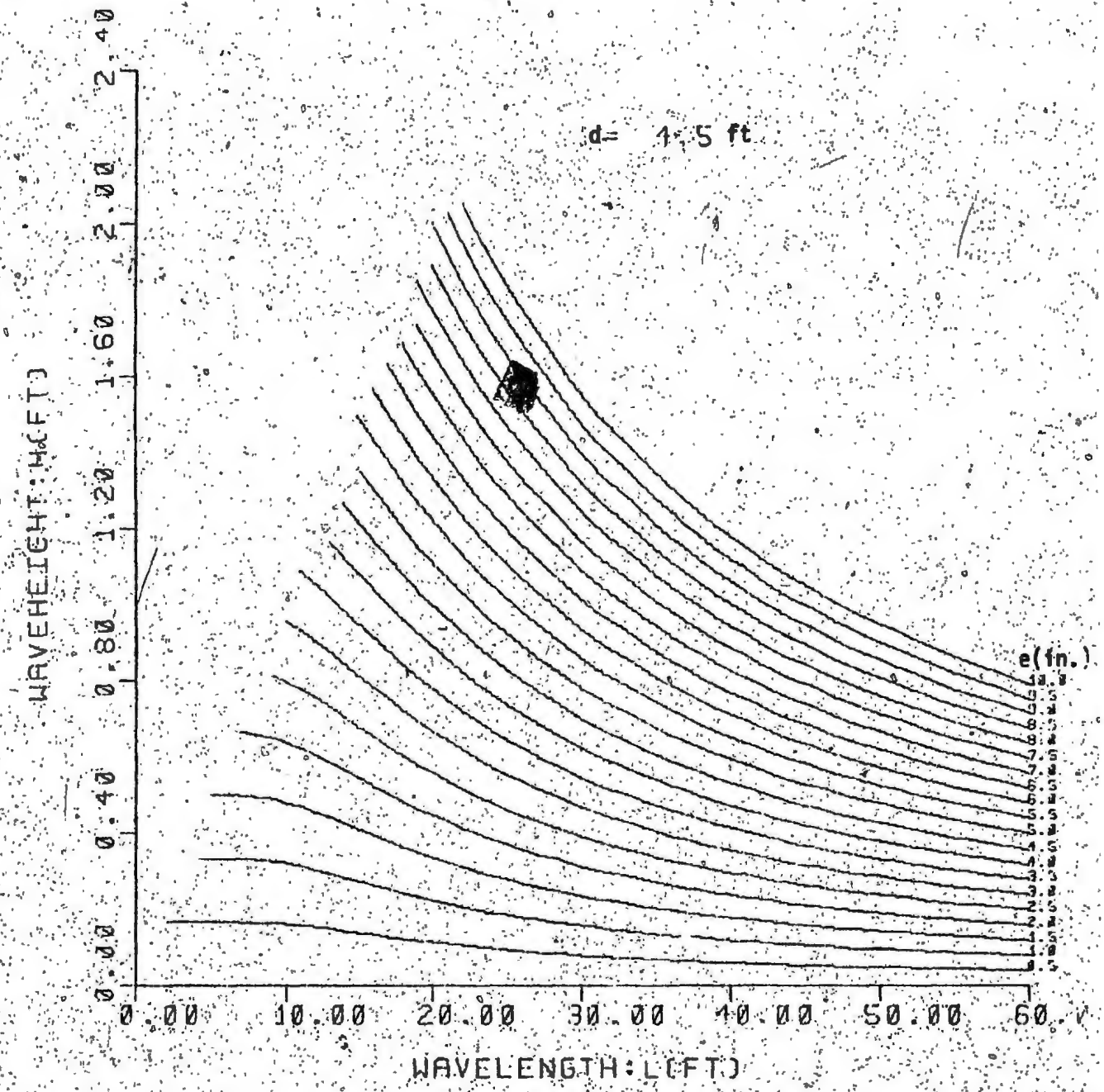

Fig. 7: Theoretical Performance Envelope for 4.5 ft Water Depth

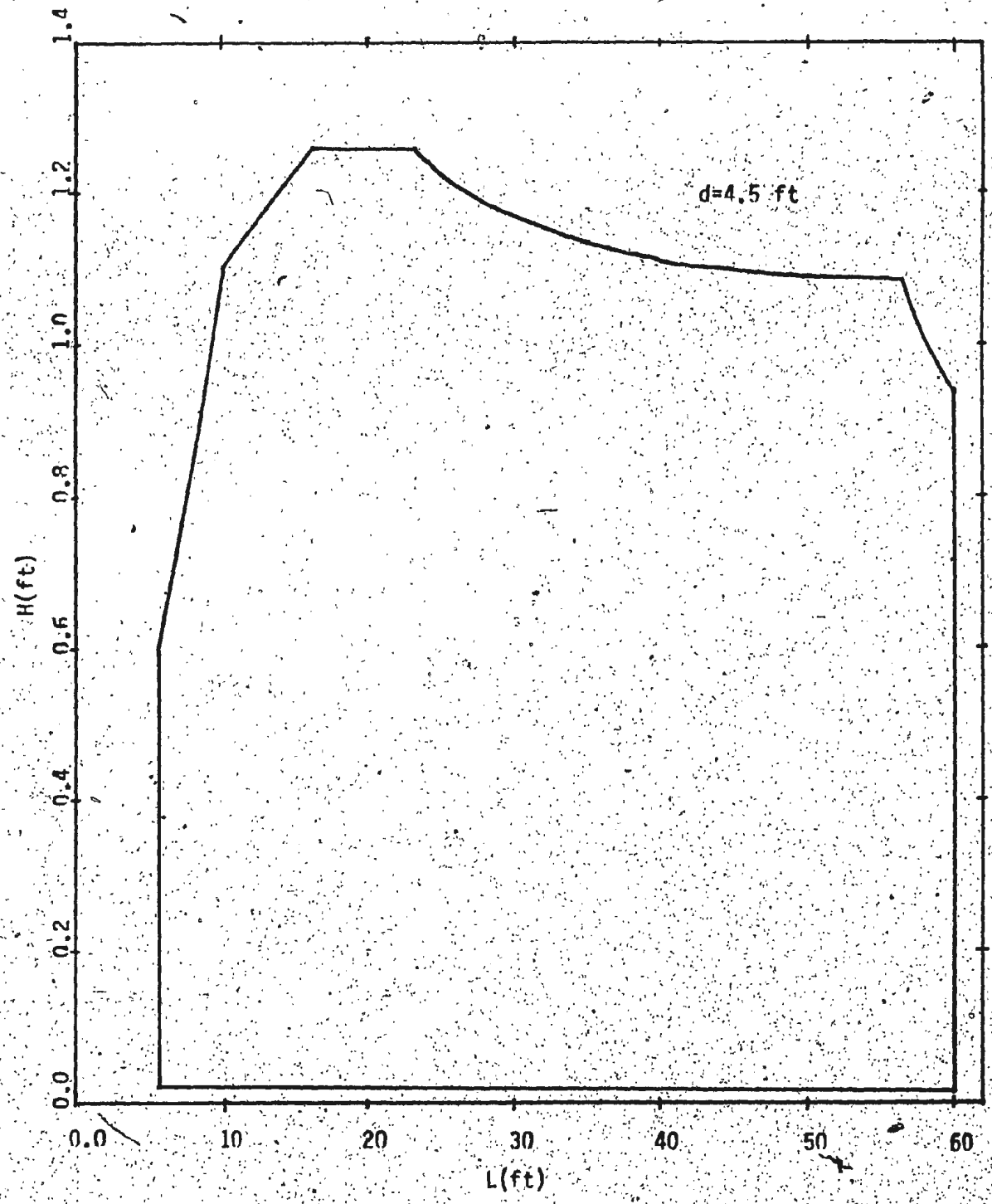

Fig. 8: Experimental Performance Envelope for 4.5 ft Water Depth

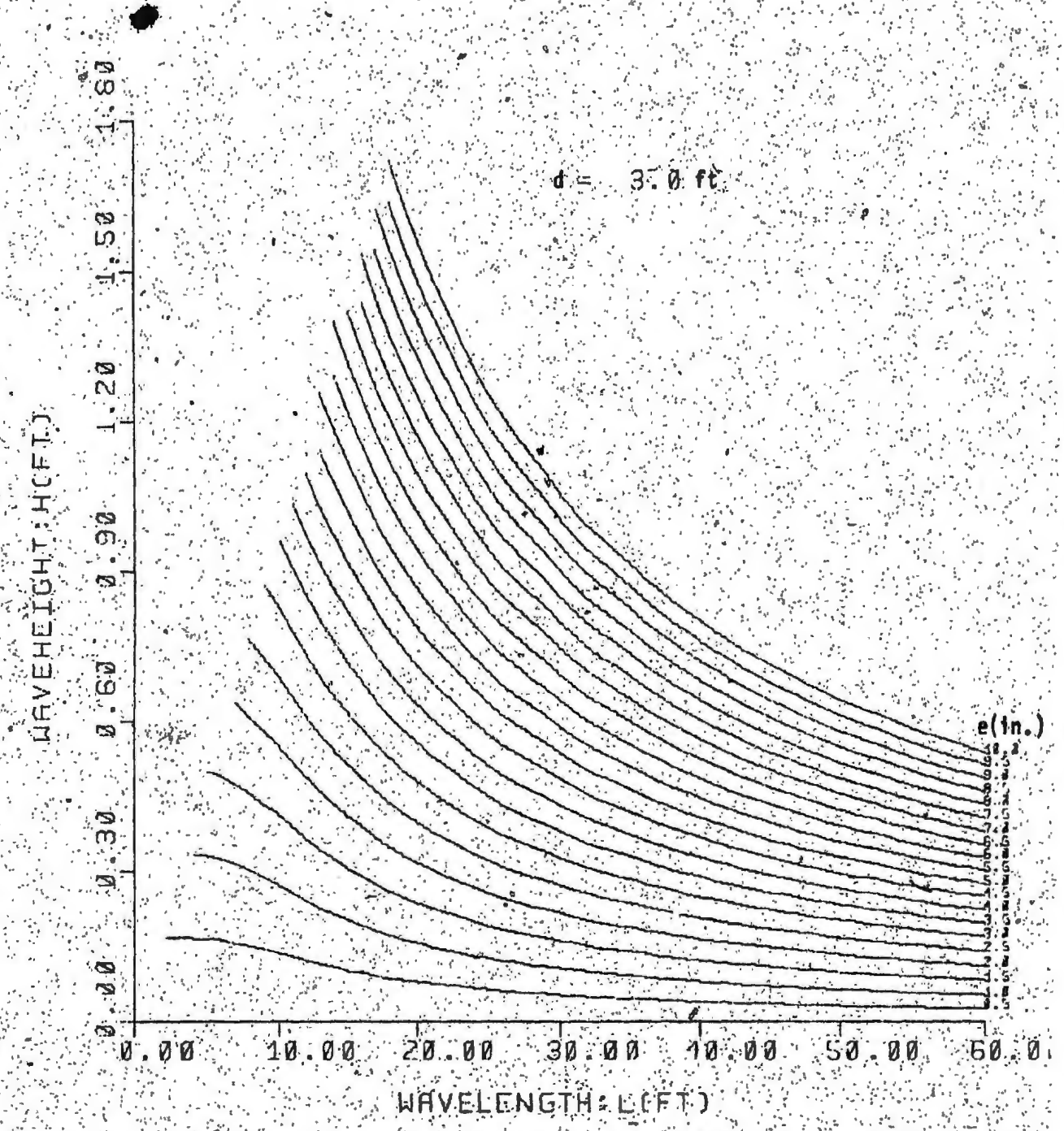

Fig. 9: Theoretical Performance Envelope for 3 ft Water Depth

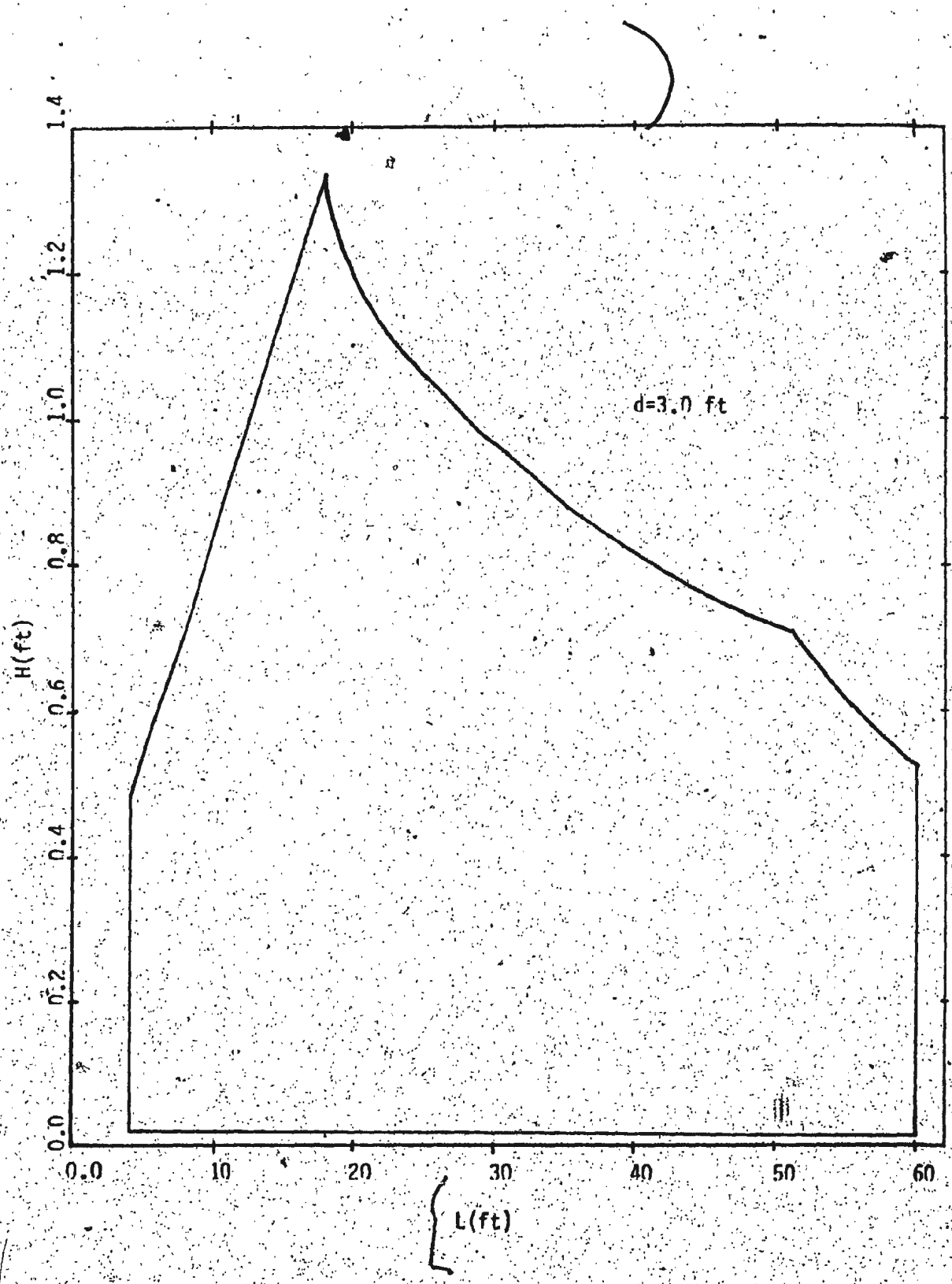

Fig. 10: Experimental Performance Envelope for 3 ft Water Depth

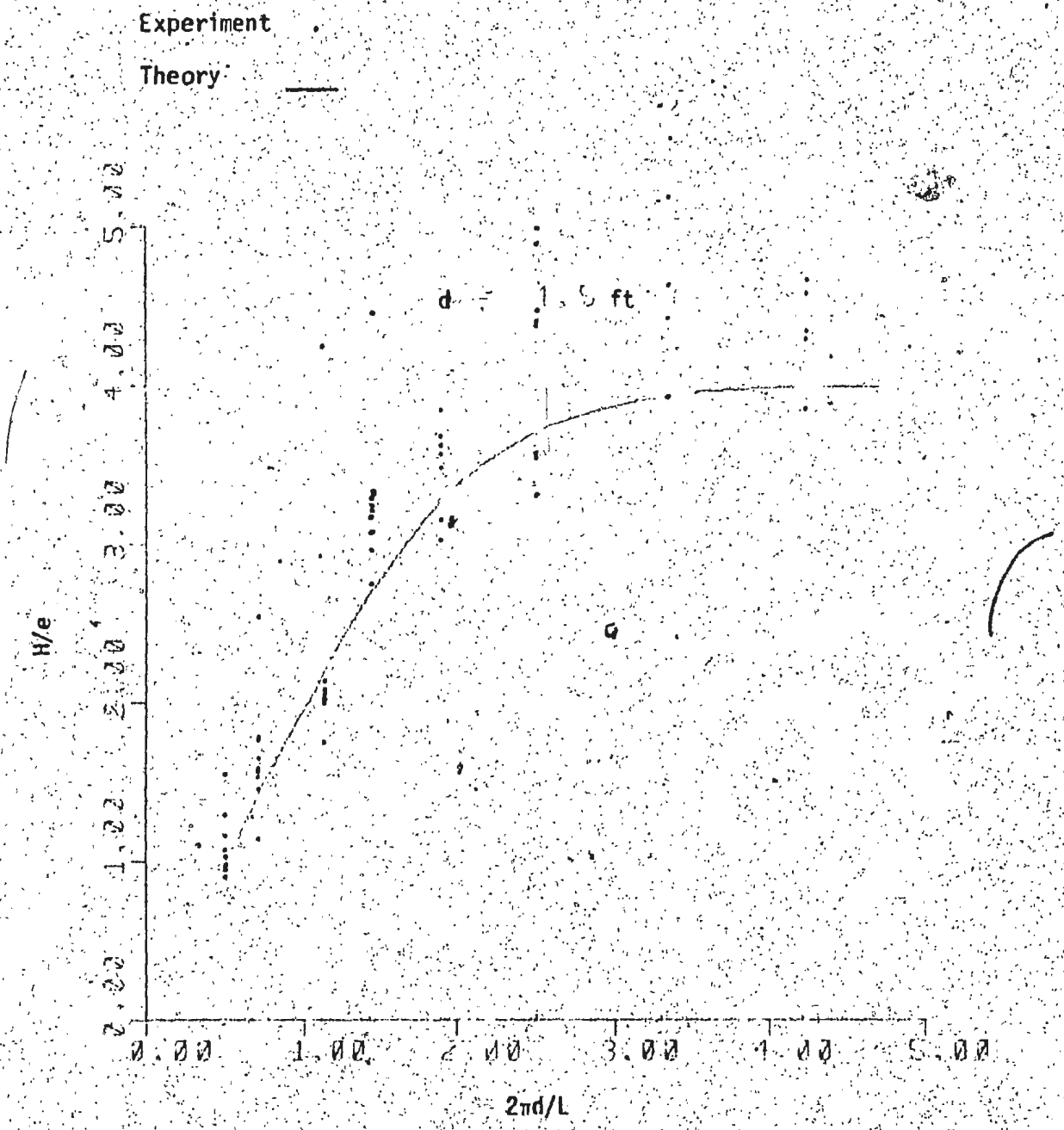

Fig. 11: Wave Generator Transfer Function for 4.5 ft Water Depth

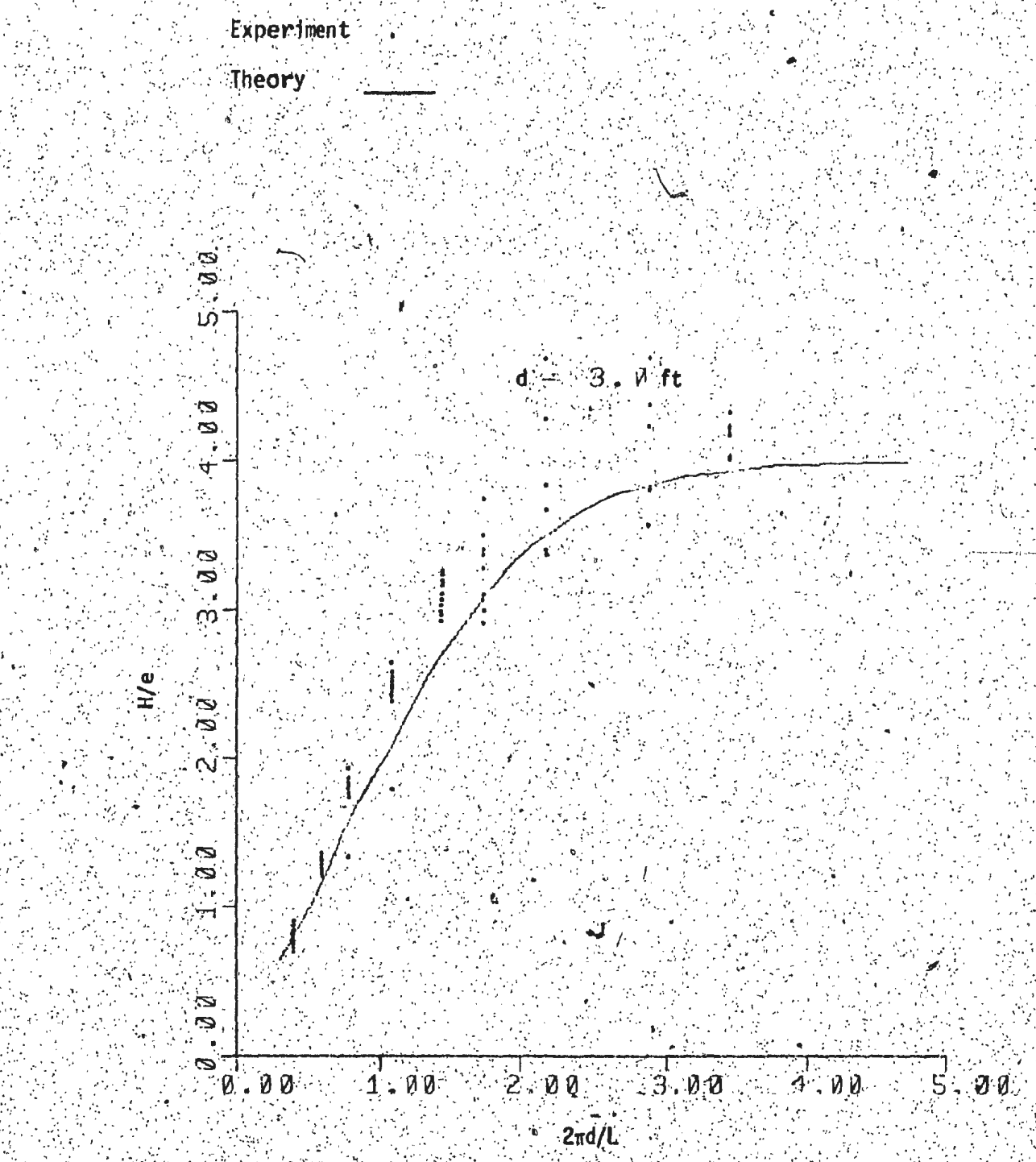

Fig. 12: Wave Generator Transfer Function for 3 ft Water Depth

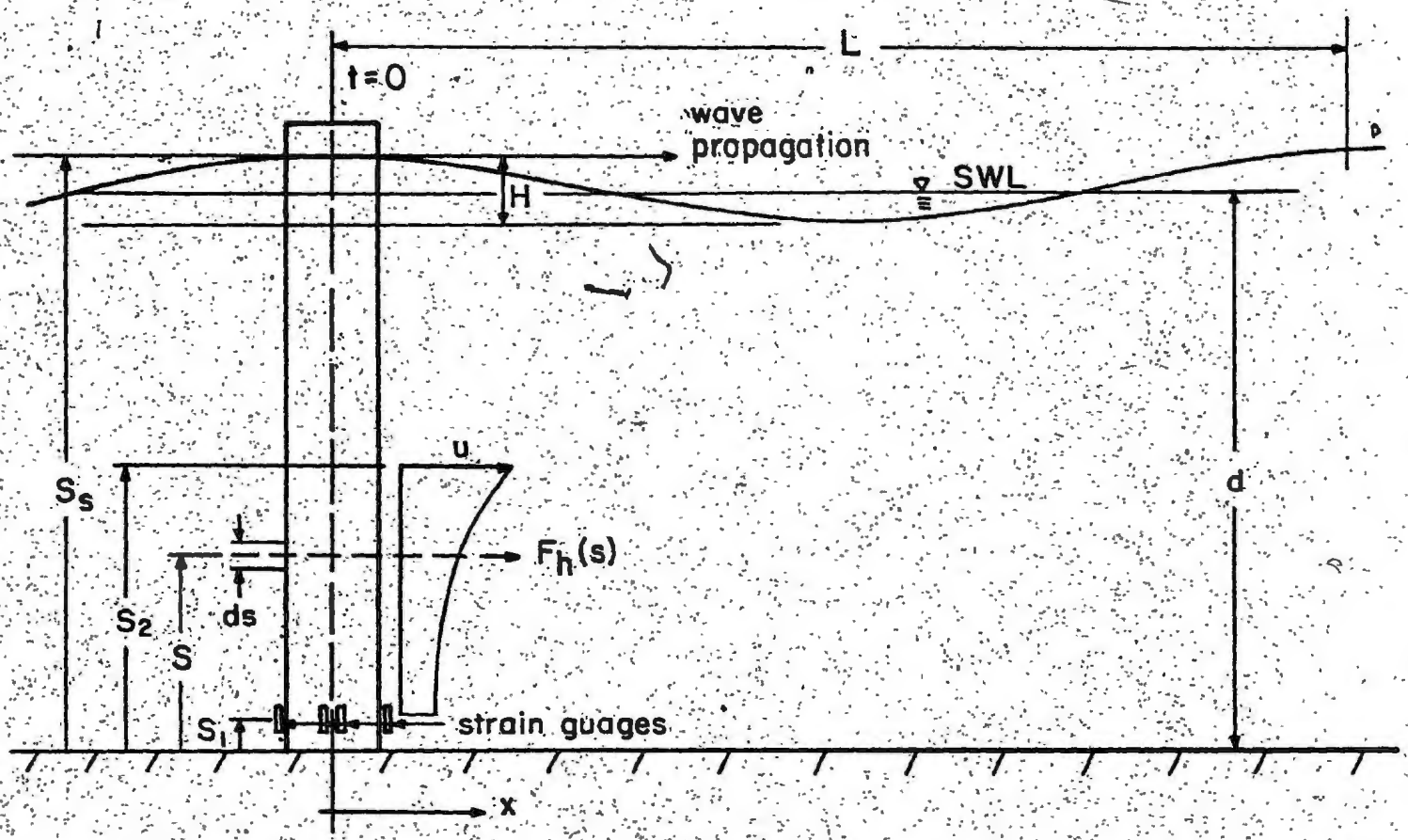

Fig. 13: Definition Sketch

Fig. 14: View of Wave Gauges Used to Measure Reflection Coefficients

Fig. 15: Calibration of Model

Fig. 16: Cylinder Under Test

Fig. 17: Vortex Shedding in the Wake of the Circular Cylinder

Fig. 18: View of Typical Output from the Strain Gage Bridges

Fig. 19: Tensile Specimen in Testing Machine

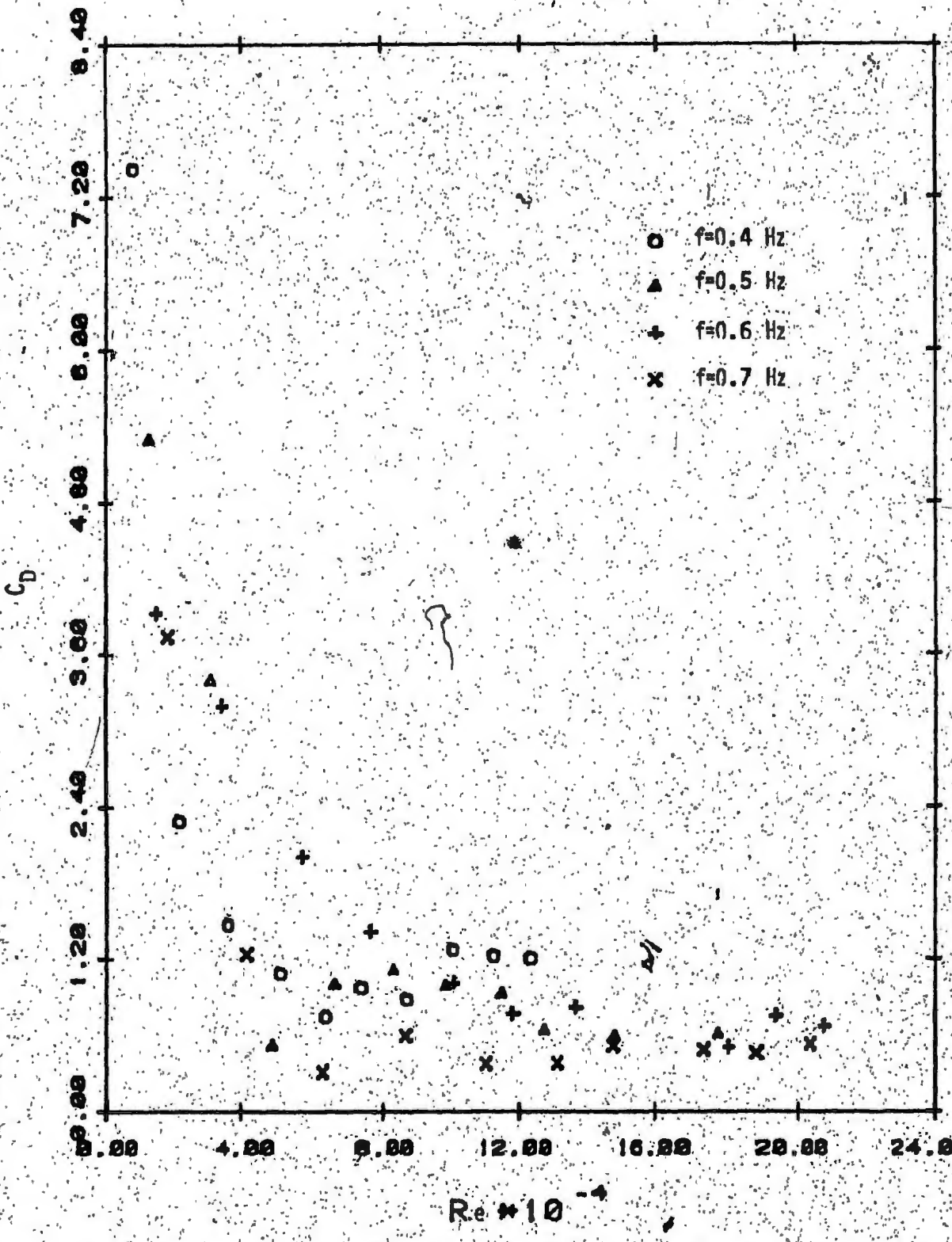

Fig. 20: Drag Coefficient vs. Reynolds Number

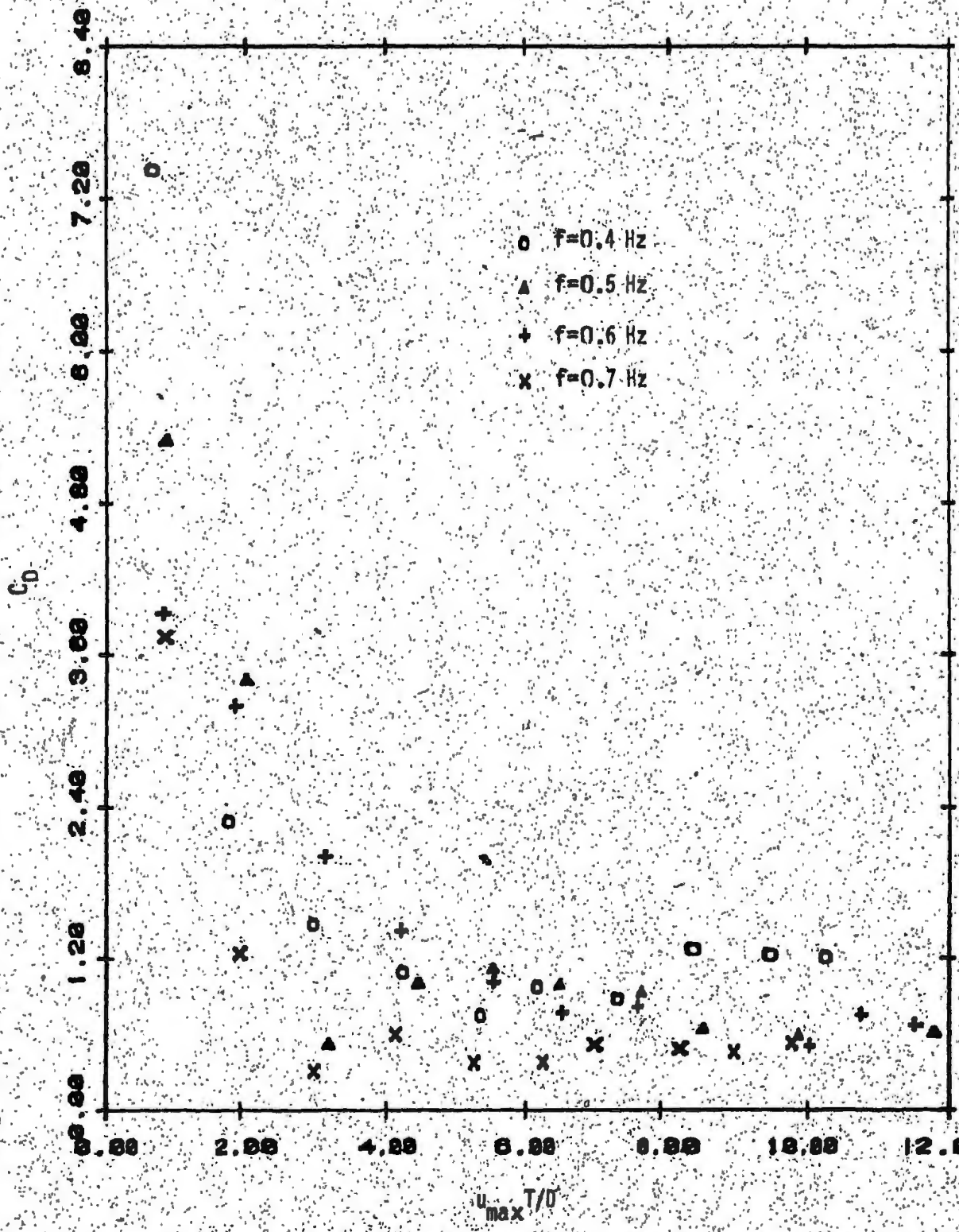

Fig. 21: Drag Coefficient vs. Keulegan-Carpenter Number

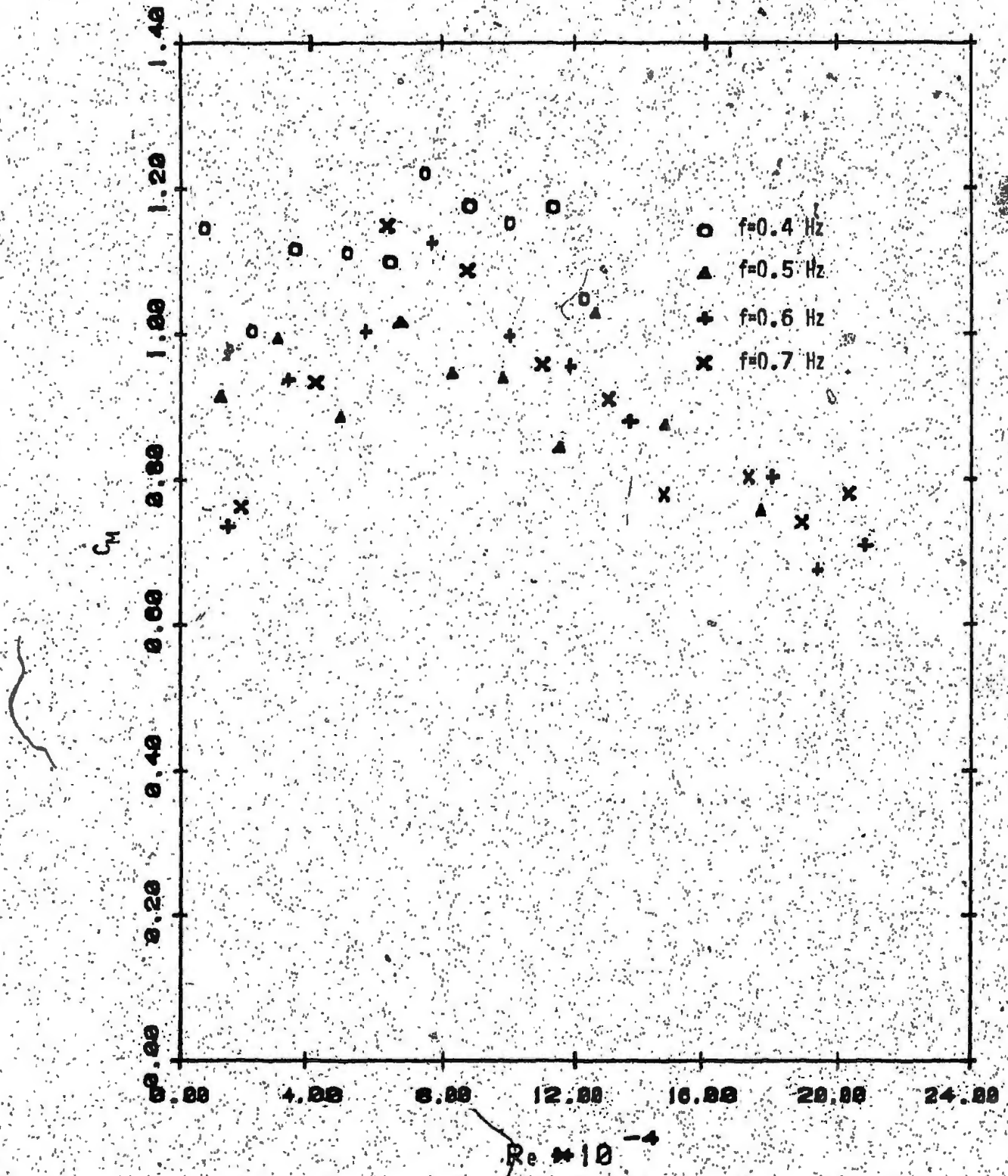

Fig. 22: Mass Coefficient vs. Reynolds Number

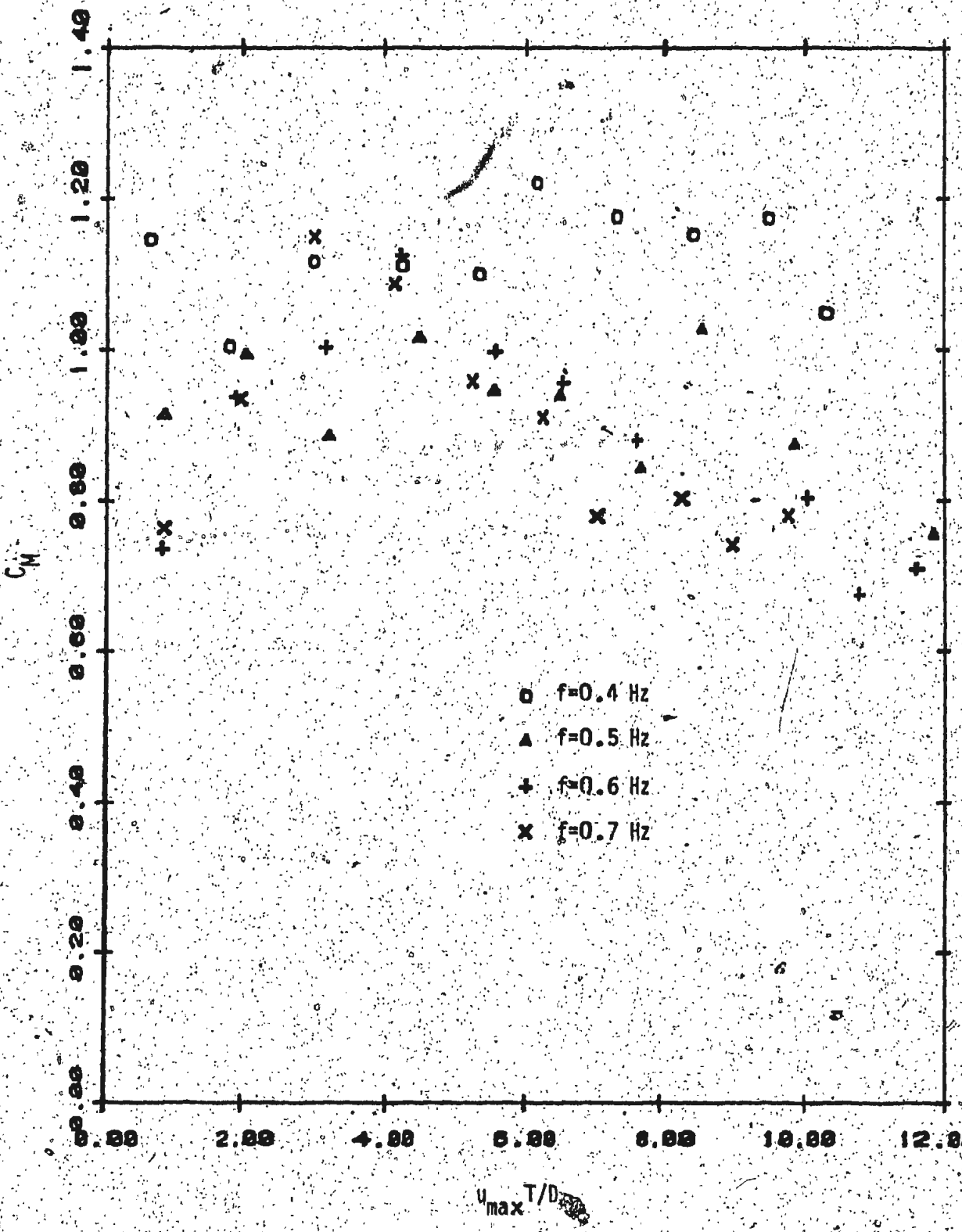

Fig. 23: Mass Coefficient vs. Keulegan-Carpenter Number

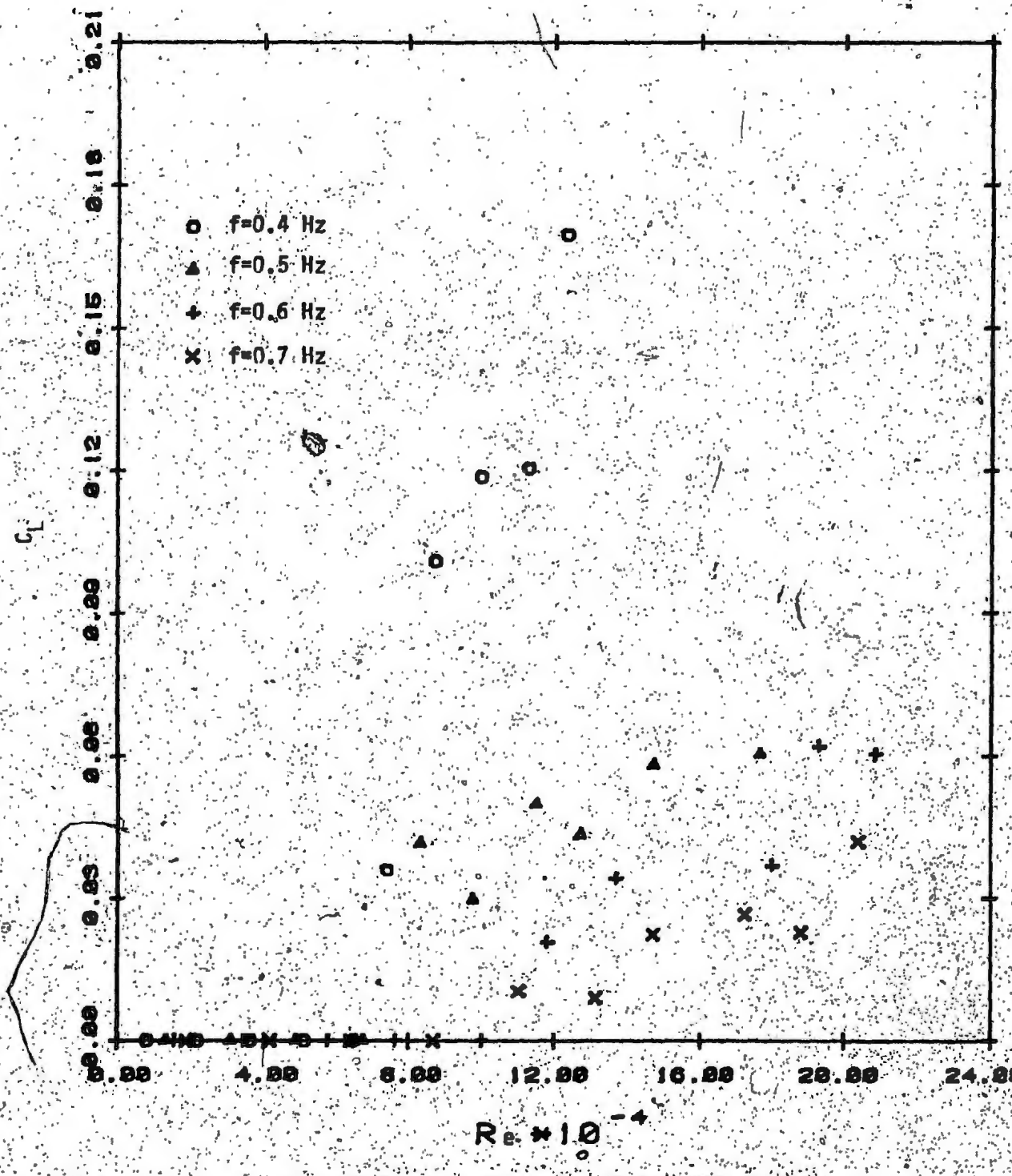

Fig. 24: Lift Coefficient vs. Reynolds Number

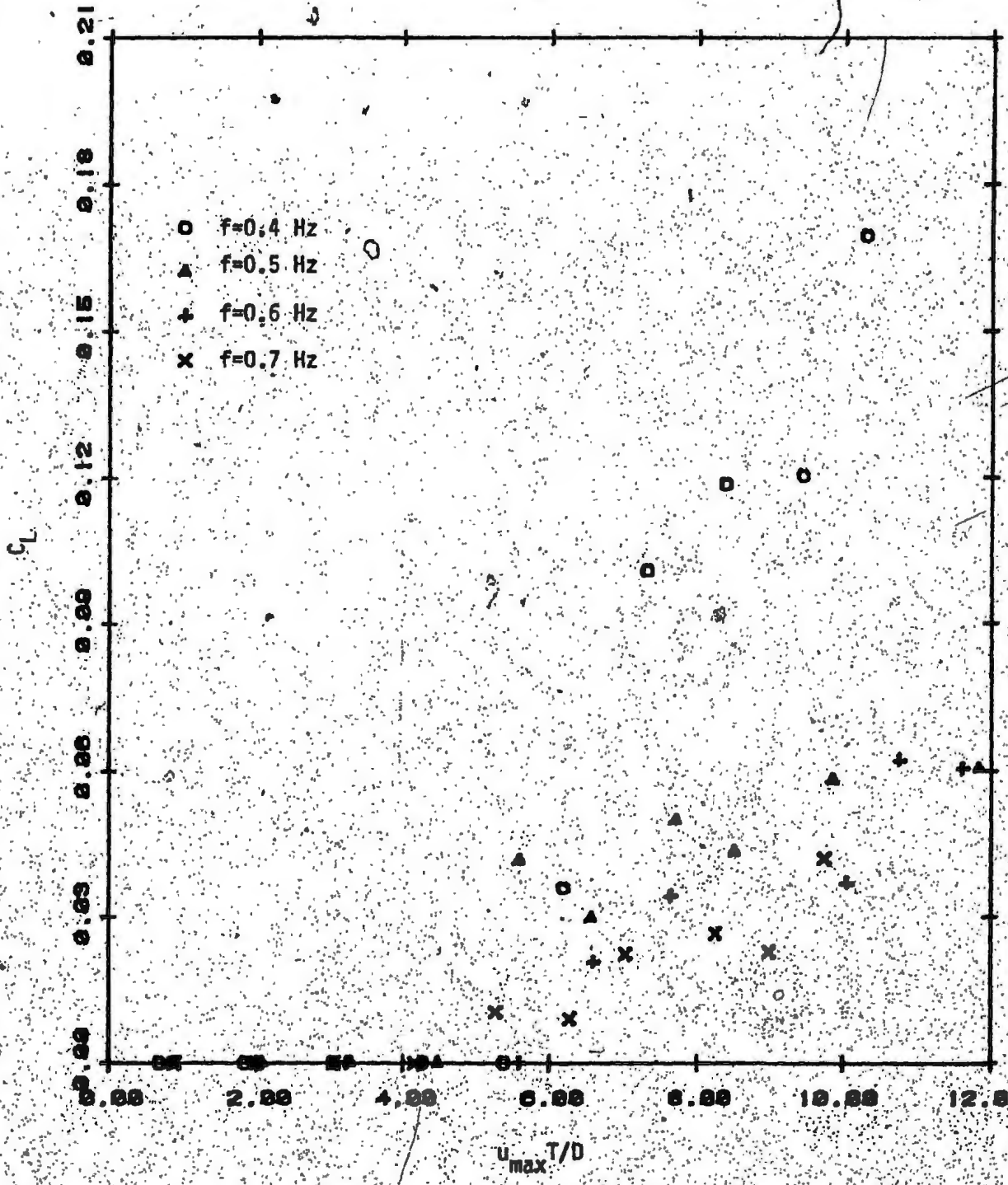

Fig. 25: Lift Coefficient vs. Keulegan-Carpenter Number

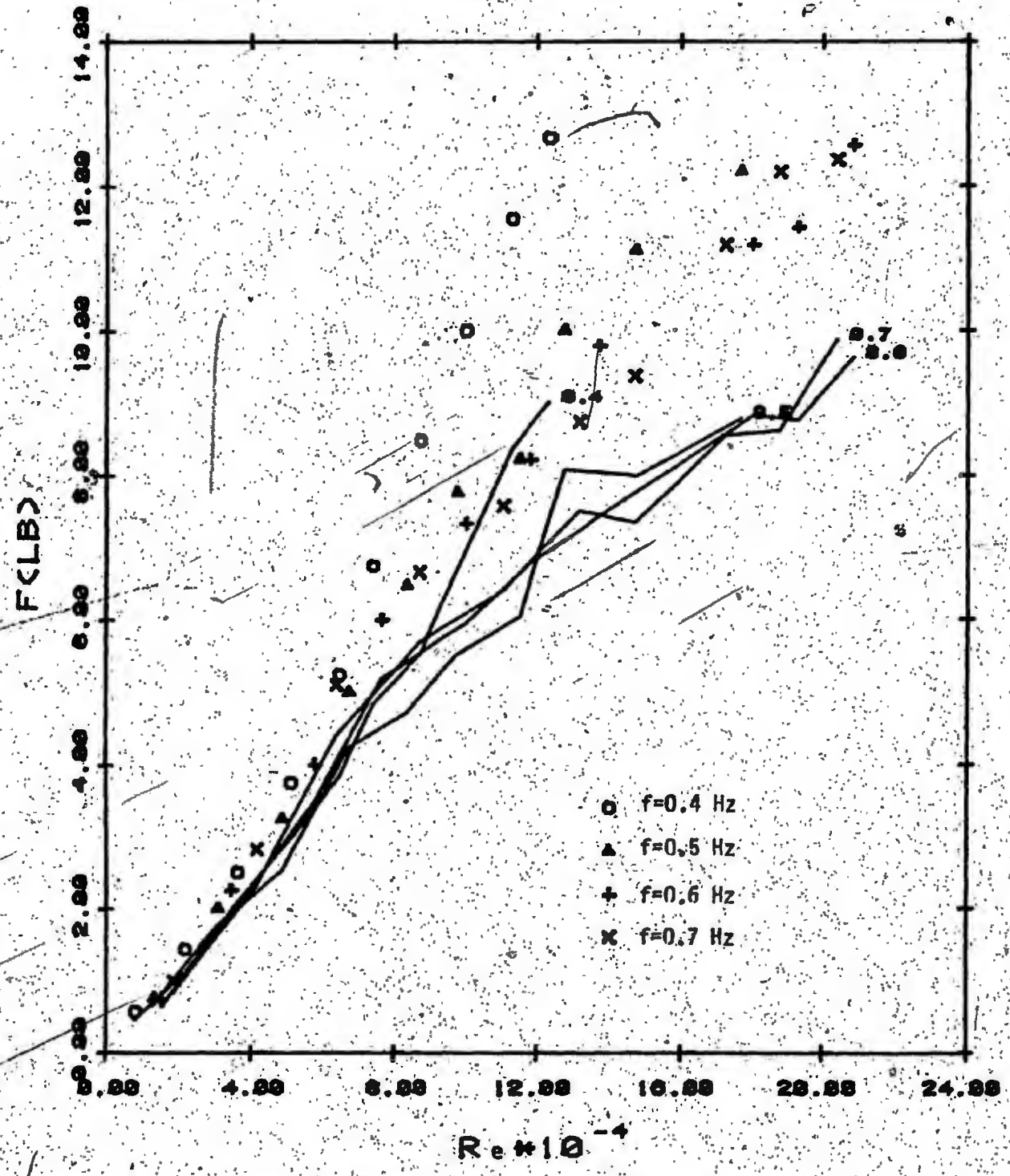

Fig. 26: Longitudinal Force vs. Reynolds Number

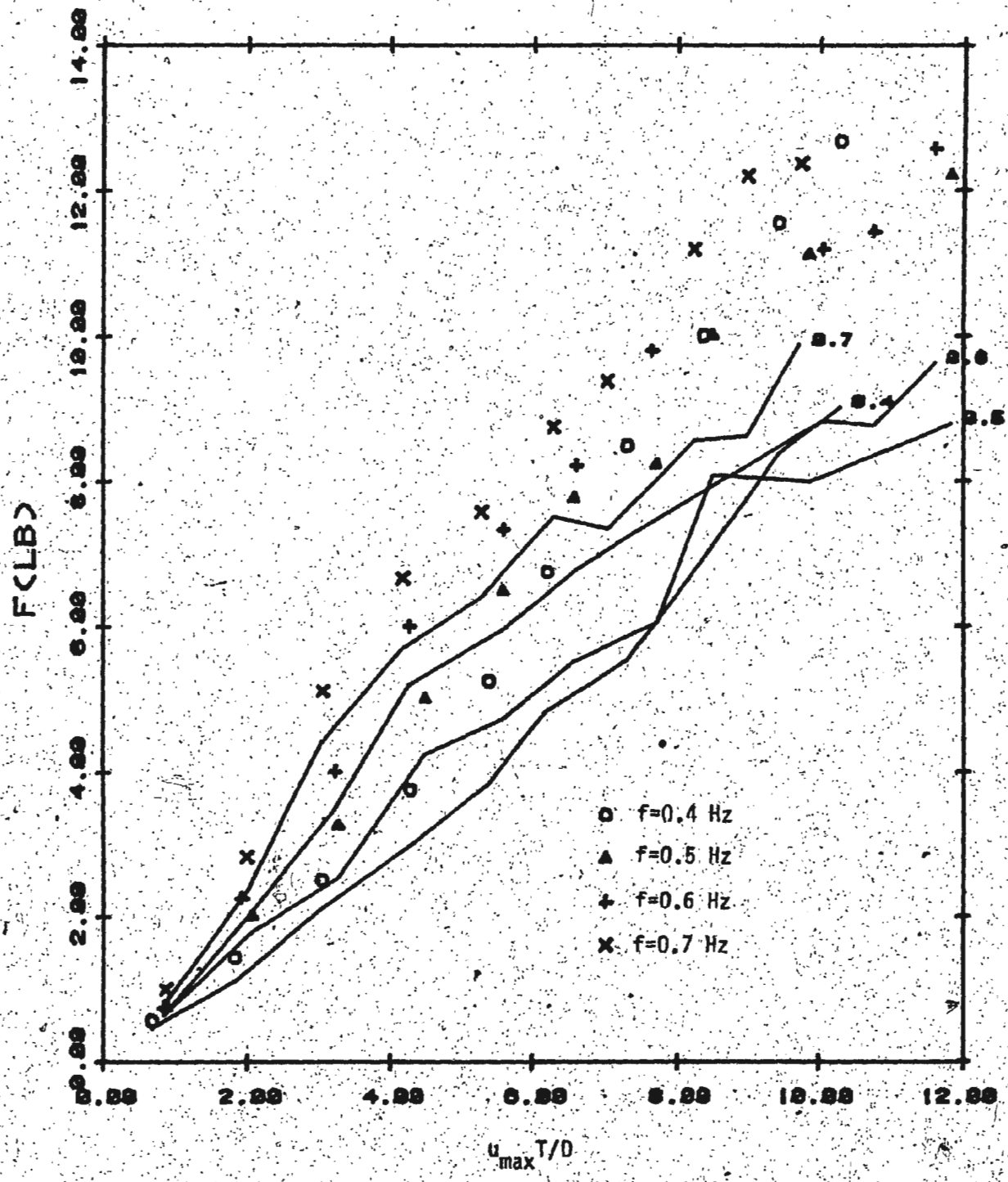

Fig. 27: Longitudinal Force vs. Keulegan-Carpenter Number

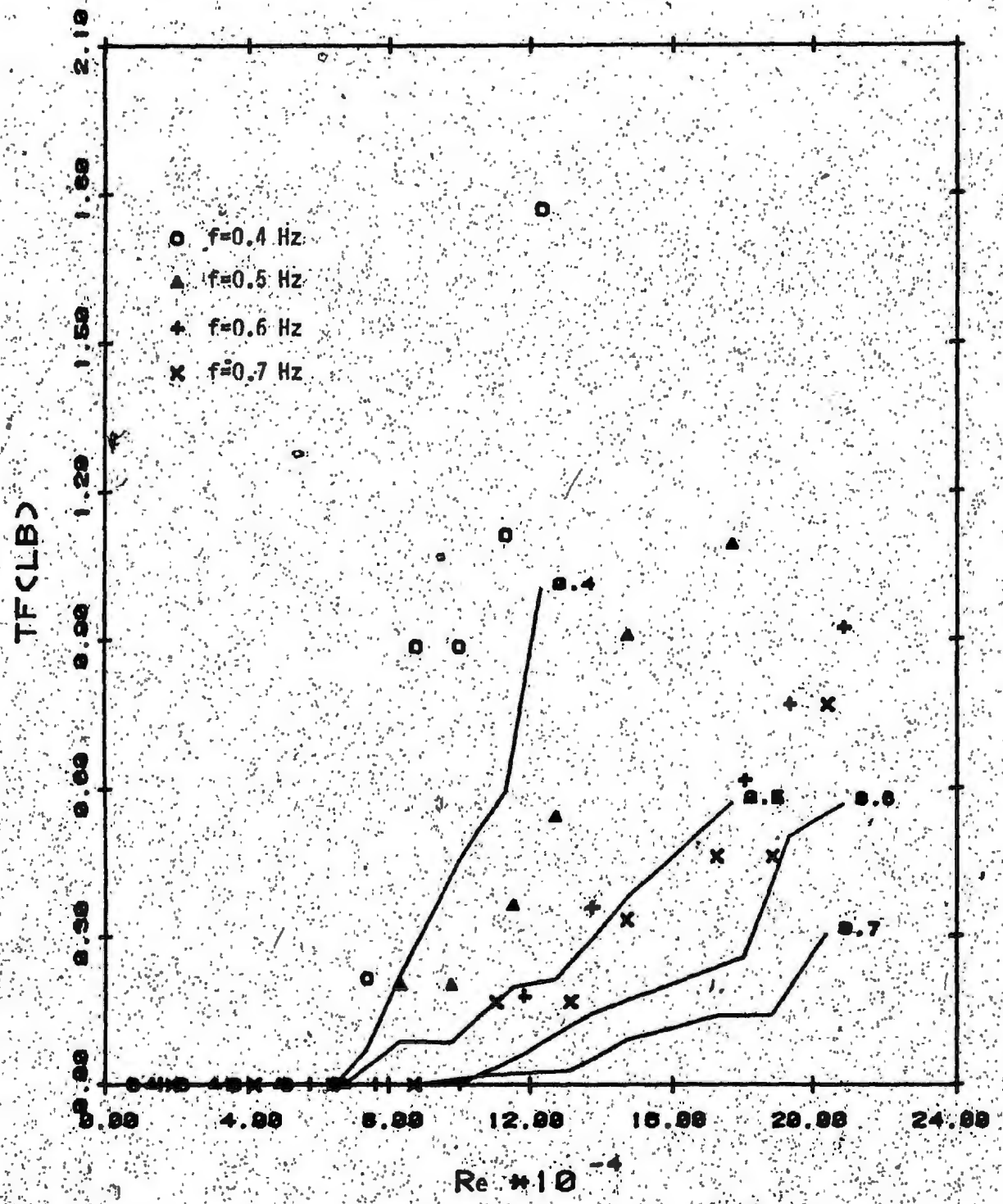

Fig. 28: Transverse Force vs. Reynolds Number

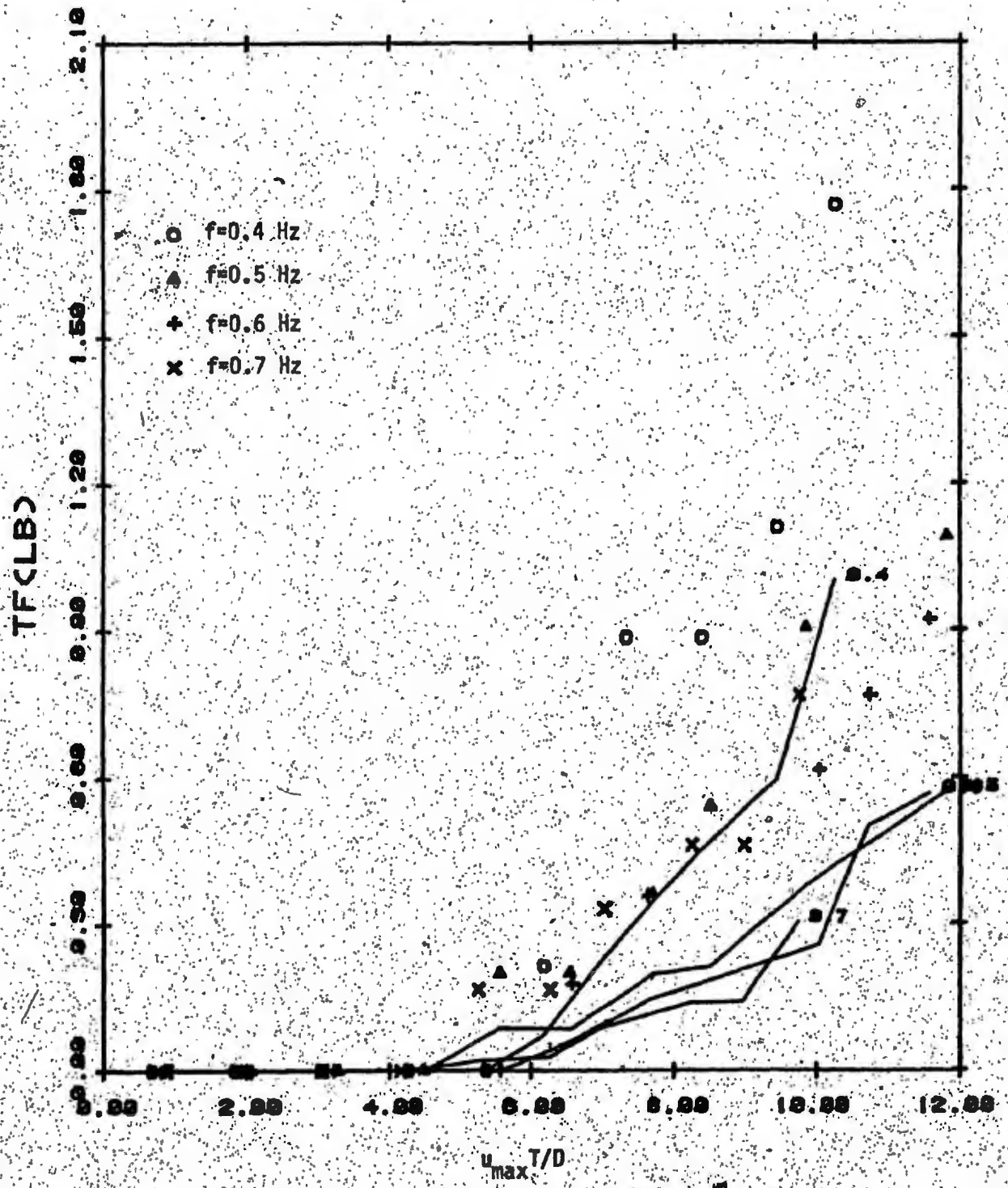

Fig. 29: Transverse Force vs. Keulegan-Carpenter Number

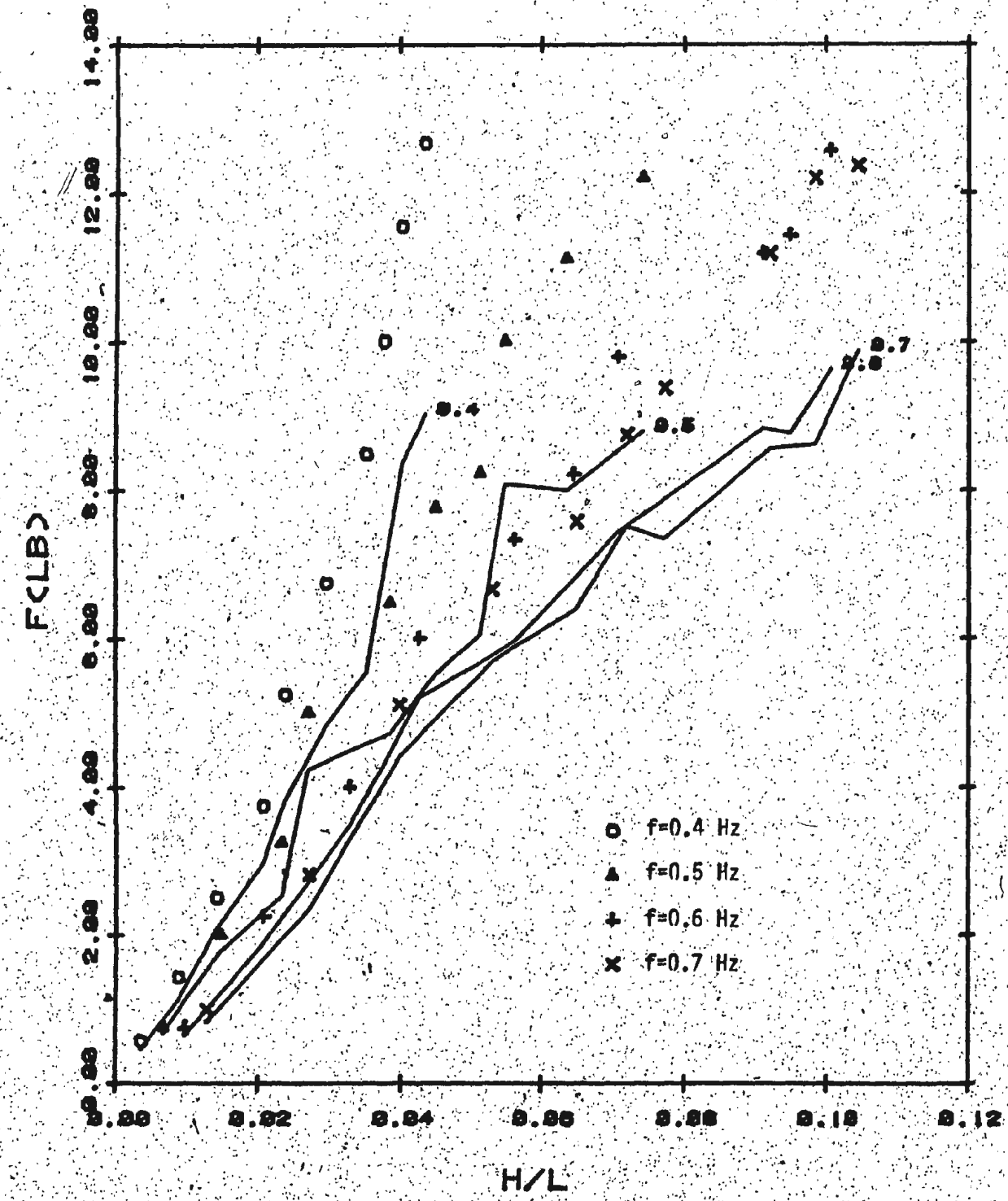

Fig. 30: Longitudinal Force vs. Wave Steepness

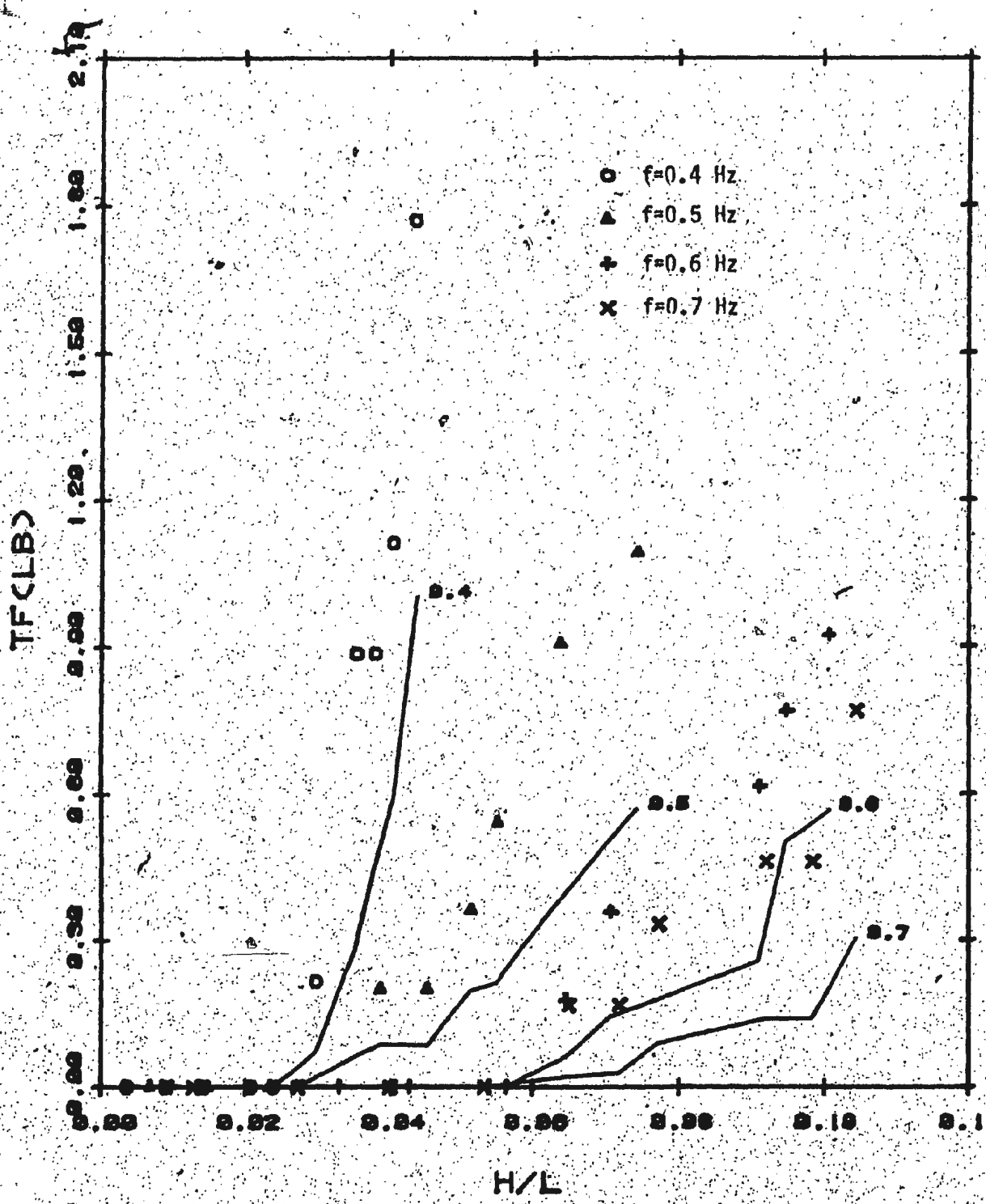

Fig. 31: Transverse Force vs. Wave Steepness

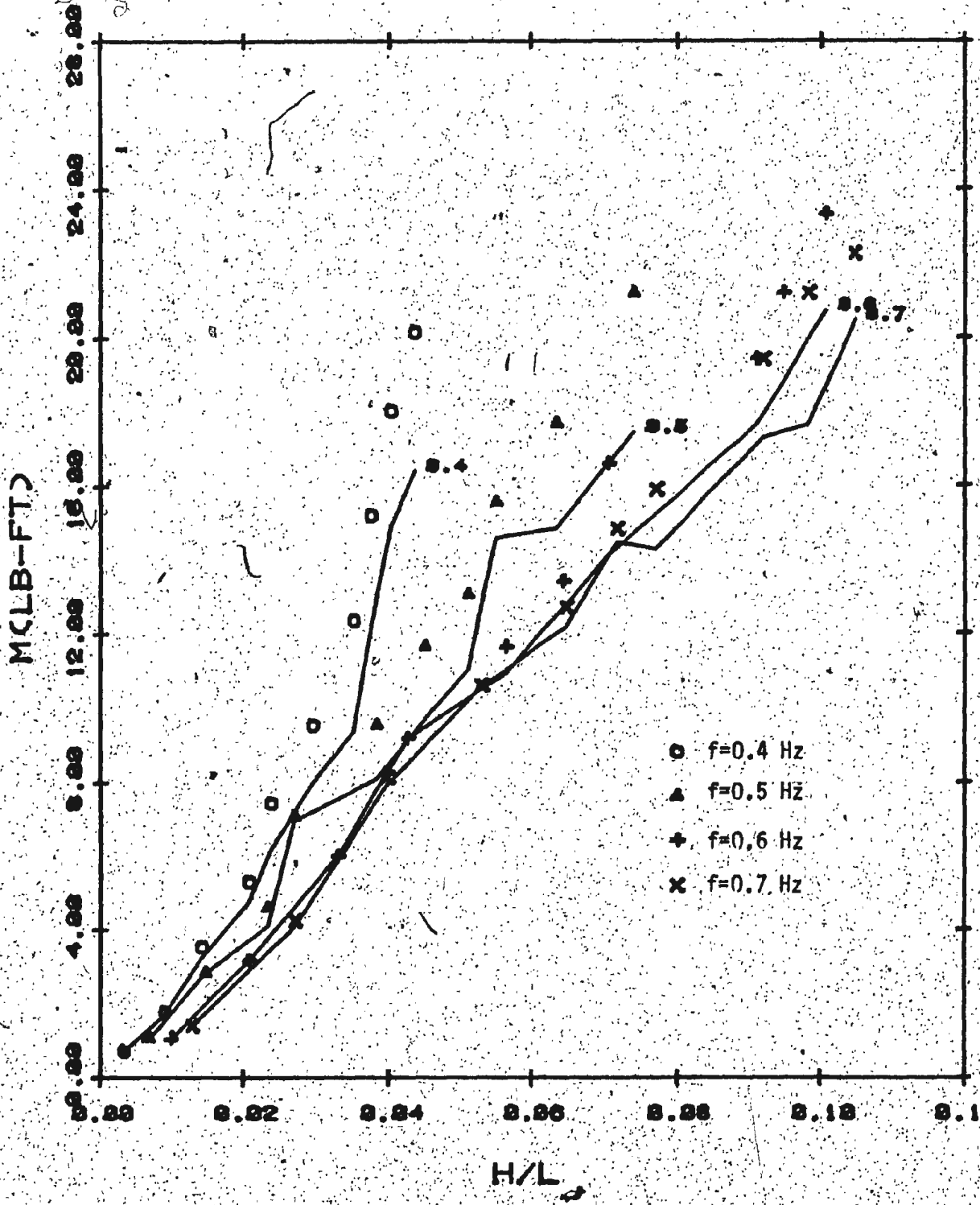

Fig. 32: Longitudinal Moment vs. Wave Steepness

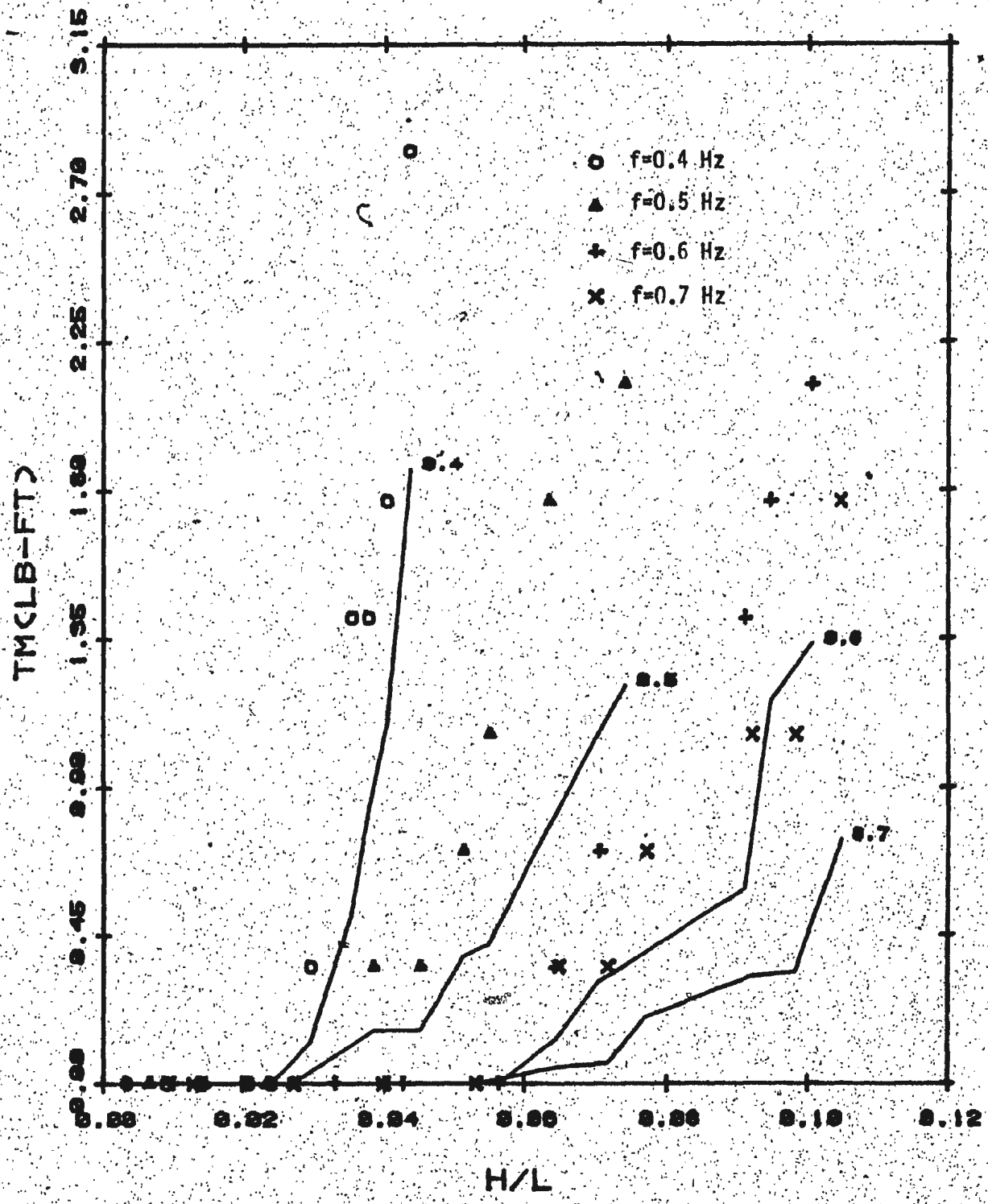

Fig. 33: Transverse Moment vs. Wave Steepness

APPENDIX A

Computer Program for the Analysis of Piston-Type Wave Generator Performance

```
$COMPILE
C       THIS PROGRAM IS BASED ON BIESEL'S THEORY FOR PISTON-TYPE
C       WAVE GENERATOR
C       H:WAVEHEIGHT(FT)
C       L:WAVELENGTH(FT)
C       D:WATER DEPTH(FT)
C       E:STROKE(INCH)
        DIMENSION L(100,120),H(100,120),XC(100,120)
        REAL L
        D=3.0
        G=6.2832*D
        PRINT 12
        DO 1 II=5,100,5
        I=II/5
        AI=II
        EE=AI/120.
        E=EE*12.
        DO 2 JJ=10,600,10
        AJ=JJ
        J=JJ/10
        L(I,J)=AJ/10.
        XC(I,J)=D/L(I,J)
        X=G/L(I,J)*2.
        IF(X.GT.174.672) GO TO 3
        EX1=EXP(X)
        EX2=EXP(-1.*X)
        EX3=EXP(X/2.)
        H(I,J)=(EX1+EX2-2.)/(EX1-EX2+4.*G/L(I,J))*4.*EE
        YP=H(I,J)/L(I,J)
        IF(YP.GT.0.1) GO TO 4
        GO TO 2
    3   H(I,J)=(EX3-2./EX3)/(EX3+4.*G/(L(I,J)*EX3))*4.*EE
        GO TO 2
    4   H(I,J)=0.
    2   CONTINUE
        PRINT 10,E
   10   FORMAT(///,1X,2HE=,F10.4,//)
        PRINT 13
   13   FORMAT(3X,1HL,6X,1HH,9(5X,1HL,6X,1HH),//)
        PRINT 11,(L(I,J),H(I,J),J=1,60)
    1   CONTINUE
   11   FORMAT(10(F5.1,F8.2))
        PRINT 12
   12   FORMAT(1H1)
        STOP
        END

$EXECUTE
```

APPENDIX B

Computer Program for the Analysis of Wave Forces and Overturning Moments on a Vertical Circular Cylinder Based on Stoke's First Order Wave Theory

```
$COMPILE
C       THIS PROGRAM IS BASED ON THE STOKES' FIRST ORDER WAVE THEORY FOR THE WAVE
C       FORCES AND MOMENTS ON THE CIRCULAR CYLINDRICAL PILE
C       F:WAVE FREQUENCY(HZ)
C       H:WAVEHEIGHT(FT)
C       L:WAVELENGTH(FT)
C       D:WATER DEPTH(FT)
C       PD:PILE DIAMETER(FT)
C       REC:RELATIVE DEPTH
C       WS:WAVE STEEPNESS
C       AT:THE RATIO OF PILE DIAMETER TO WAVELENGTH
C       UMAX:THE MAXIMUM HORIZONTAL COMPONENT OF PARTICLE VELOCITY(FT/SEC)
C       UTD:THE KEULEGAN AND CARPENTER PARAMETER
C       RD:REYNOLDS NUMBER
C       NU:KINEMATIC VISCISITY(FT**2/SEC)
C       CD:DRAG COEFFICIENT
C       CM:MASS COEFFICIENT
C       CL:LIFT COEFFICIENT
C       IN:MOMENT OF INERTIA(INCH**4)
C       E:YOUNG'S MODULUS(PSI)
C       RO:MASS DENSITY OF WATER(SLUG/FT**3,LB-SEC**2/FT**4)
C       S1:ANY POINT FROM THE BOTTOM OF OCEAN(FT)
C       MF:MEASURING HORIZONTAL FORCE IN THE LONGITUDINAL DIRECTION(LB)
C       MTF:MEASURING HORIZONTAL FORCE IN THE TRANSVERSE DIRECTION(LB)
C       FH:THEORETICAL HORIZONTAL FORCE IN THE LONGITUDINAL DIRECTION(LB)
C       TF:THEORETICAL HORIZONTAL FORCE IN THE TRANSVERSE DIRECTION(LB)
C       EBS:LONGITUDINAL STRAIN(E-06)
C       EBSD:LONGITUDINAL STRAIN(E-06) FOR DRAG COEFFICIENT
C       EBSM:LONGITUDINAL STRAIN(E-06) FOR MASS COEFFICIENT
C       EBT:TRANSVERSE STRAIN(E-06)
C       EBTL:TRANSVERSE STRAIN(E-06) FOR LIFT COEFFICIENT
C       MM:MEASURABLE MOMENT AT POINT S1 IN THE LONGITUDINAL DIRECTION(LB-FT)
C       M1:MEASURABLE MOMENT AT POINT S1 FOR THE DRAG COEFFICIENT
C       M2:MEASURABLE MOMENT AT POINT S1 FOR MASS COEFFICIENT
C       MR:MEASURABLE MOMENT AT POINT S1 IN THE TRANSVERSE DIRECTION(LB-FT)
C       M3:MEASURABLE MOMENT AT POINT S1 FOR THE LIFT COEFFICIENT
C       MT:THEORETICAL MOMENT AT POINT S1 IN THE LONGITUDINAL DIRECTION(LB-FT,)
C       TM:THEORETICAL MOMENT AT POINT S1 IN THE TRANSVERSE DIRECTION(LB-FT)
C       BHM:THE PHASE ANGLE OFTHE MAXIMUM TOTAL MOMENT WILL BE OCCURRED(DEGREES)
C       BHF:THE PHASE ANGLE OF THE MAXIMUM TOTAL HORIZONTAL FORCE WILL BE
C      OCCURRED(DEGREES)
C       L1:THE LOCATION OF THE APPLICATION OF THE RESULTANT HORIZONTAL FORCE IN
C       THE LONGITUDINAL DIRECTION(FT)
C       L2:THE LOCATION OF THE APPLICATION OF THE RESULTANT HORIZONTAL FORCE IN
C       THE TRANSVERSE DIRECTION(FT)
      1       DIMENSION UTD(40),RD(40),F(40),H(40),L(40),MM(40),MT(40),UMAX(40),
     6FH(40),BHM(40),BHF(40),CD(40),CM(40),L1(40),EBS(40),IK(40),
     5REC(40),WS(40),AT(40),AF(40),EBT(40),MR(40),CL(40),TF(40),TM(40),
     2L2(40),MF(40),MTF(40),EBSD(40),EBSM(40),EBTL(40),M1(40),M2(40),
     3M3(40)
      2       REAL L,NU,MM,MT,IN,K1,K2,K3,K4,L1,MR,L2,MF,MTF,M1,M2,M3
      3       D=3.
      4       PD=0.547
      5       NU=0.00001
      6       RO=2.
      7       PI=3.1416
      8       IN=27.41
      9       E=507300.
     10       C=3.28125
     11       S1=0.23
```

```
      DO 15 I=1,40
   15 READ(5,7) MF(I),MTF(I)
      DO 10 I=1,40
      IK(I)=I
      READ(5,1)F(I),H(I),L(I),EBS(I),EBT(I)
      READ(5,50)EBSD(I),EBSM(I),EBTL(I)
      S2=H(I)/2.+D
      X1=2.*PI*S2/L(I)
      X2=2.*PI*D/L(I)
      RED(I)=D/L(I)
      WS(I)=H(I)/L(I)
      AT(I)=PD/L(I)
      AF(I)=D*F(I)**2
      COSH1=(EXP(X1)+EXP(-X1))/2.
      SINH1=(EXP(X2)-EXP(-X2))/2.
      UMAX(I)=PI*H(I)*F(I)*COSH1/SINH1
      UTD(I)=UMAX(I)/(F(I)*PD)
      RD(I)=UMAX(I)*PD/NU
      R1=2.*PI*S1/L(I)
      R12=2.*R1
      R22=2.*X1
      SINH2=(EXP(X1)-EXP(-X1))/2.
      SINH3=(EXP(R22)-EXP(-R22))/2.
      SINH4=(EXP(R1)-EXP(-R1))/2.
      SINH5=(EXP(R12)-EXP(-R12))/2.
      COSH2=(EXP(X1)+EXP(-X1))/2.
      COSH3=(EXP(R22)+EXP(-R22))/2.
      COSH4=(EXP(R1)+EXP(-R1))/2.
      COSH5=(EXP(R12)+EXP(-R12))/2.
      K1=(R22-R12+SINH3-SINH5)/(16.*SINH1**2)
      K2=(SINH2-SINH4)/SINH1
      K3=(1./(64.*SINH1**2))*(0.5*(R22)**2-0.5*(R12)**2+R22*SINH3-R12*
     7SINH5-COSH3+COSH5)
      K4=(1./(2.*SINH1))*(X1*SINH2-R1*SINH4-COSH2+COSH4)
      MM(I)=E*EBS(I)*IN/(12.*C)
      M1(I)=E*EBSD(I)*IN/(12.*C)
      M2(I)=E*EBSM(I)*IN/(12.*C)
      CD(I)=M1(I)/(RO*PD*(F(I)*H(I)*L(I))**2*(K3-R1*K1/2.))
      CM(I)=(4.*M2(I))/(PI*H(I)*RO*(F(I)*L(I)*PD)**2*(K4-R1*K2/2.))
      PMC=ABS(PI*PD*CM(I)*(K4-R1*K2/2.)/(8.*H(I)*CD(I)*(K3-R1*K1/2.)))
      IF(PMC.GT.1.) GO TO 20
      GO TO 21
   20 PMC=1.
   21 BHMR=ARSIN(PMC)
      BHM(I)=180./PI*BHMR
      PMD=ABS(PI*PD*CM(I)*K2/(8.*H(I)*CD(I)*K1))
      IF(PMD.GT.1.) GO TO 22
      GO TO 23
   22 PMD=1.
   23 BHFR=ARSIN(PMD)
      BHF(I)=180./PI*BHFR
      FH(I)=PI*RO*PD*(F(I)*H(I))**2*L(I)*(PI*PD/(4.*H(I))*CM(I)*K2*SIN(
     2BHFR)+CD(I)*K1*ABS(COS(BHFR))*COS(BHFR))
      MT(I)=RO*PD*(F(I)*H(I)*L(I))**2*(PI*PD/(4.*H(I))*CM(I)*K4*SIN(BHMR
     3)+CD(I)*K3*ABS(COS(BHMR))*COS(BHMR)-R1*(PI*PD/(8.*H(I))*CM(I)*
     4K2*SIN(BHMR)+0.5*CD(I)*K1*ABS(COS(BHMR))*COS(BHMR)))
      L1(I)=MT(I)/FH(I)
      MR(I)=E*EBT(I)*IN/(12.*C)
      M3(I)=E*EBTL(I)*IN/(12.*C)
      CL(I)=M3(I)/(RO*PD*(F(I)*H(I)*L(I))**2*(K3-R1*K1/2.))
```

```
      TF(I)=PI*RO*PD*(F(I)*H(I))**2*L(I)*CL(I)*K1
      TM(I)=RO*PD*(F(I)*H(I)*L(I))**2*CL(I)*(K3-F1*K1/2.)
      IF(TF(I).EQ.0.) GO TO 12
      L2(I)=TM(I)/TF(I)
      GO TO 10
   12 L2(I)=0.
   10 CONTINUE
      WRITE(6,2)
      DO 5 I=1,40
    5 WRITE(6,3)IK(I),F(I),H(I),L(I),RED(I),WS(I),AT(I),AF(I),UMAX(I),
     8UTD(I),RD(I),MM(I),CD(I),CM(I)
      WRITE(6,9)
      DO 6 I=1,40
    6 WRITE(6,11)IK(I),BHM(I),BHF(I),MT(I),FH(I),MF(I),L1(I),MR(I),
     9CL(I),TF(I),MTF(I),TM(I),L2(I)
      WRITE(6,68)
    1 FORMAT(F5.1,2F10.3,2E15.2)
   50 FORMAT(3E15.2)
    2 FORMAT(1H1,6X,1HF,5X,1HH,6X,1HL,8X,3HD/L,5X,3HH/L,5X,4HPD/L,4X,6HD
     1*F**2,1X,4HUMAX,8X,3HUTD,9X,2HRD,11X,2HMM,5X,2HCD,7X,2HCM,//)
    3 FORMAT(I5,F5.1,6F8.3,3E12.4,3F8.3)
    7 FORMAT(2F10.3)
    9 FORMAT(1H1,8X,3HBHM,7X,3HBHF,7X,2HMT,8X,2HFH,8X,2HMF,9X,2HL1,8X,
     12HMR,8X,2HCL,8X,2HTF,8X,3HMTF,7X,2HTM,8X,2HL2,//)
   11 FORMAT(I5,12F10.3)
   68 FORMAT(1H1)
      STOP
      END
```

$EXECUTE